Recent advances on bioactive baghdadite ceramic for bone tissue engineering applications: 20 years of research and innovation (a review)

Sorour Sadeghzade [a,*], Jingyi Liu [a], Huiru Wang [a], Xin Li [a], Jinrui Cao [a], Huiling Cao [b], Bin Tang [c], Hongyan Yuan [a,**]

[a] Shenzhen Key Laboratory of Soft Mechanics & Smart Manufacturing, Department of Mechanics and Aerospace Engineering, Southern University of Science and Technology, Shenzhen, 518055, China
[b] Department of Biochemistry, School of Medicine, Southern University of Science and Technology, Shenzhen, 518055, China
[c] Department of Biomedical Engineering, Southern University of Science and Technology, Shenzhen, 518055, China

ABSTRACT

Various artificial bone graft substitutes based on ceramics have been developed over the last 20 years. Among them, calcium-silicate-based ceramics, which are osteoconductive and can attach directly to biological organs, have received great attention for bone tissue engineering applications. However, the degradation rate of calcium-silicate and bone formation is often out of balance, resulting in stress shielding (osteopenia). A new strategy to improve the drawbacks of these ceramics is incorporating trace elements such as Zn, Mg, and Zr into their lattice structures, enhancing their physical and biological properties. Recently, baghdadite ($Ca_3ZrSi_2O_9$) ceramic, one of the most appealing calcium-silicate-based ceramics, has demonstrated high bioactivity, biocompatibility, biodegradability, and cell interaction. Because of its physical, mechanical, and biological properties and ability to be shaped using various fabrication techniques, baghdadite has found high potential in various biomedical applications such as coatings, fillers, cement, scaffolds, and drug delivery systems. Undoubtedly, there is a high potential for this newly developed ceramic to contribute significantly to therapies to provide a tremendous clinical outcome. This review paper aims to summarize and discuss the most relevant studies performed on baghdadite-based ceramics and composites by focusing on their behavior in vivo and in vitro.

1. Introduction

During the past decades, millions of people worldwide have suffered from bone-related diseases caused by accidents, trauma, degenerative diseases, infections, and cancers. About 2.2 million orthopedic surgeries, including bone grafting, are performed annually, with at least 500 thousand surgeries just in the USA [1]. Common treatments using autografts/allografts (gold standard methods) have numerous limitations, including limited donor disease transmission, immunological reactions, donor site morbidity, infection risk, and foreign body rejection [1–3]. Various synthetic materials, particularly bioceramics, have been developed to overcome these limitations as synthetic bone grafting in various forms, such as scaffolds, cement, spheres, and bulk [4–6].

Among all these ceramics, baghdadite has been acknowledged as a bioceramic with superior biological and mechanical features (compared to the other calcium-silicate-based ceramic), close to natural bone

[7–10]. It is well-known that the composition of baghdadite is one of the key parameters affecting its properties and determining its biocompatibility, bioactivity, and biodegradability. This ceramic has received significant attention in the recent decade due to its demonstrated ability to efficiently stimulate osteogenesis and treat large-size bone defects by releasing bioactive ionic products [11]. Due to this significant advantage, baghdadite has great potential to be widely used for the repair and regeneration of bone tissues [11–13]. Baghdadite ceramic features prominently among established biomaterials for the replacement or regeneration of the musculoskeletal system and dental applications. This ceramic accelerates the healing time, prevents implant rejection, and improves cell migration, adhesion, proliferation, differentiation, new bone formation and vascularization [14]. Furthermore, baghdadite forms strong biological binding to bone tissue in vivo and has been developed as an alternative replacement to metallic implants in low load-bearing applications [15–17]. Also, some studies have consistently
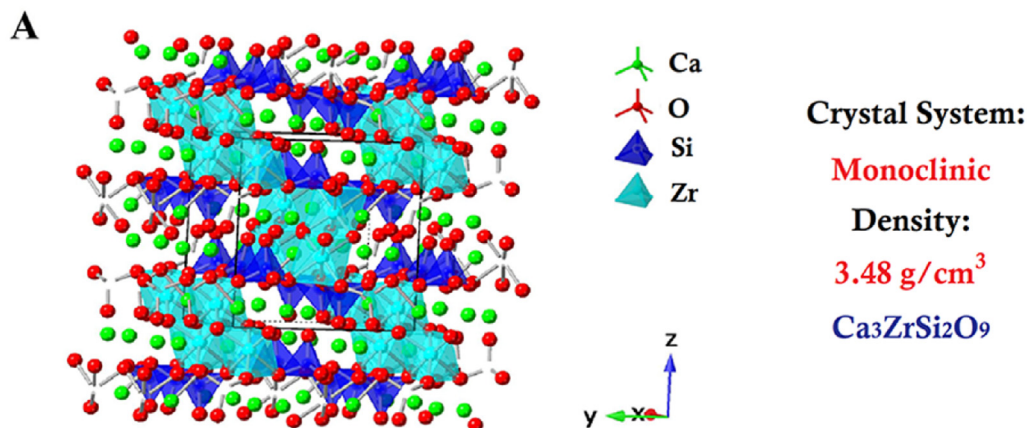
---

demonstrated that surface modification of metallic implants with baghdadite substantially affects the expression of osteogenic genes of bone cells in vitro [18].

Further studies have indicated that a significant aspect of baghdadite
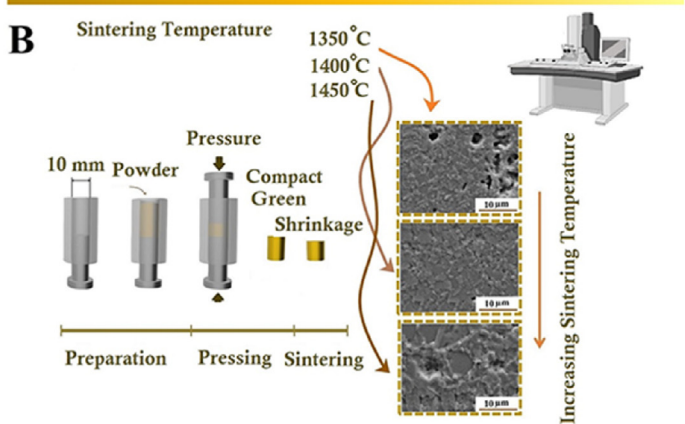
ceramic is its ability to release ions at a sufficient concentration that stimulates osteoblast proliferation and differentiation [5,19,20].

Additionally, baghdadite ceramic and its modification through incorporation of various elements, including zinc (Zn), strontium (Sr),

Fig. 1. (A) Baghdadite crystal structure, fabrication procedure and microstructure of (B) sintered bulk baghdadite ceramic at various sintering temperature, SEM images reproduced with permission from Ref. [38], baghdadite scaffold fabrication procedure by (C) polymer sponge method, SEM image reproduced with permission from Ref. [11], (D) space holder methods, SEM image reproduced with permission from Ref. [8], and (E) freeze-drying, SEM image reproduced with permission from Ref. [39].

and bismuth (Bi), and composites of these ceramics, influence their biological response, antibacterial properties, mechanical strength for load-bearing applications [21–24].

Despite various studies showing the ability of baghdadite to integrate with bone tissue and exhibit competitive biological and mechanical properties with calcium phosphate ceramics, the application of this ceramic is due to its inherent brittleness [8,25]. Its low resistance to the initiation and propagation of cracks means it can often be used as granules or as porous scaffolds in non-load-bearing applications. Compared to other calcium silicate-based ceramics (except diopside ceramic), baghdadite suggests higher bioactivity, pH controllability, X-ray mass attenuation coefficient, biocompatibility and toughness. These observations refer to the lattice structure of baghdadite ceramic. Incorporating the third element (Zr^{4+} ion) into the structure of the calcium-silicate ceramic can improve or control the chemical stability, bioactivity, and mechanical properties of baghdadite. As a matter of fact, similar to Ti and Si (like sphene and wollastonite ceramics), Zr is a quadrivalent ion. It has the potential to build a network that ionically binds Ca ions, enhancing baghdadite's stability compared to other calcium silicate ceramics [26].

Since 2008, several researchers have published studies concerning medical applications of this ceramic, with the majority focused on recent years (2018–2021) [18,27–33]. A literature review of publications in the ScienceDirect database using keywords such as "baghdadite as bioceramic" and "baghdadite as biomaterial" did not show a comprehensive overview discussing and comparing their properties and potential for biomedical purposes. This current review studies all aspects of either pure or composite baghdadite bioceramic and provides an overview of baghdadite as a bioceramic for bone tissue engineering applications between 2000 and 2022. In the current work, we described the goals of exploring the structure, mechanical, physical, and biological characteristics of synthetic baghdadite ceramic and its applications in the biomedical sector. Especially in this study, we focus on the interaction of this ceramic in pure or composite forms with various cell types and in vivo findings in small or big animals for human therapies and disease modelling. We also discuss key considerations and decisions during the materials design pathway and outline the most promising fabrication techniques, such as 3D printing. Finally, we highlight future approaches and challenges in developing this ceramic in bone tissue engineering.

2. Pure baghdadite ceramic

2.1. Characteristics of crystallographic structure

The baghdadite ($Ca_3ZrSi_2O_9$) crystal structure is monoclinic, as shown in Fig. 1A, and belongs to the $CaO–ZrO_2–SiO_2$ system [30]. For the first time, baghdadite was discovered in Qala-Dizeh, Iraq, associated with banded diorite by Hermezi et al. [34]. Baghdadite is a member of the cuspidine group, a series of silicates with a general formula $M_4(Si_2O_7)X_2$, in which M is a cation with a varied charge and ionic radii that are typically coordinated by octahedral space, and X can be OH, F, O. As shown in Fig. 1A, baghdadite exhibits ZrO_6 with six Zr–O distances ranging from 1.97 Å to 2.2 Å [35,36]. These minerals are composed of two types of modules. The first is a module consisting of four columns of octahedral walls that stretch along [001], and the second consists of disilicate groups. The octahedral walls are constructed with the same corner-sharing structure in this mineral family. Different orthosilicates can be linked to the octahedral walls that possess various unit cells and symmetry patterns. Their second characteristic involves the crystal chemistry of ionic distribution inside the polyhedron [35]. The parameters of the crystal structure of baghdadite are derived from Ref. [37]. Those parameters consist of a = 7.26 Å, b = 10.173 Å, c = 10.45 Å, and β = 90.87°, as well as the symmetry of the crystal is characterized by the space group $P2_1/c$.

In baghdadite ceramic, Zr plays a significant role in the physiological and mechanical properties. The durability and structural stability of calcium-silicate-based ceramics increase with the incorporation of the Zr

ion, which is a quadrivalent ion and can be linked to Ca ions [40]. This ion is normally present in human bone and tissues at a trace level in the range of 2–20 mg/kg body weight, with an estimated average daily intake in humans of 3.5 mg. The toxicity of Zr has been assessed as low to moderate in animals. It has been shown that Zr ions in baghdadite ceramic can be released in more controllable concentrations in the range of 10–100 μM into solutions simulated body fluids compared to ZrO_2 ceramic [41].

Based on the literature, the in vitro toxicity of Zr on the osteoblast-like cell line MG63 showed toxicity in the millimolar concentration range [42]. However, Zr ions have shown different behavior on the proliferation and differentiation of osteoblast-like cells at lower, more clinically relevant concentrations [41]. Zr ions can promote the proliferation and differentiation of human osteoblasts in vitro. This effect is associated with and may be mediated by the up-regulation of BMP2 expression and increased BMP signalling. Also, this ion has a novel osteogenic activity on primary human osteoblasts, enhancing their differentiation into osteoblasts and mineralized bone matrix. The mechanism for this observation is related to OPN, BSP, and osteocalcin markers which are enhanced by Zr ions up-regulating between days 3–7 of culture [41].

As mentioned before, in addition to the physical and mechanical properties of baghdadite, this ceramic also possesses superior biological properties. Compared to pure wollastonite, baghdadite shows more controllable degradation and, consequently, a more stable structure, ideal for cell culture and healing large bone defects. Numerous studies have revealed that baghdadite ceramic can support osteoblasts, osteoclasts, and endothelial cell growth and differentiation [43,44]. As mentioned in the literature [27], Zr-incorporated ceramic may have a crucial function in boosting the proliferation of bone marrow stromal cells (BMSCs). It has been reported that baghdadite shows the capability of inducing angiogenesis in biological conditions. A much lower degradation rate of the Zr-ions provides a relatively stable surface to support stem cell proliferation when incorporated into a Ca–Si-based ceramic [44]. As a result of its exceptional biological properties, baghdadite ceramic (as filler, matrix, and coating) is at the center of extensive research in the biomedical materials field. This ceramic has shown an emerging area of biocomposite materials research due to its remarkable properties [27,30,38,45–54]. The following sections will discuss the latest biomedical applications of baghdadite ceramics, the process of bioactivity mechanisms, and their behavior in vitro and in vivo conditions.

2.2. Synthesize of baghdadite powder ceramic

Natural baghdadite contains impurities like Ti ions [48]. Pure synthetic baghdadite ceramic has been produced using various fabrication methods, including ball mill [55], and sol-gel [11,56,57]. Pure baghdadite ceramic, potentially used as a bioceramic, was synthesized for the first time by Hala Zreiqa's research group at the University of Sydney in 2008 [57]. They synthesized pure baghdadite powders using a sol-gel process with zirconia oxide nitrate, calcium nitrate tetrahydrate, and tetraethyl orthosilicate. The mixture was maintained at 60 °C for 24 h and dried at 100 °C for 24 h to obtain the dry gel. Subsequently, the dry gel was calcined at 1150 °C for 3 h (mean crystallite size of 10 nm). The sintering temperature is a significant parameter for obtaining pure ceramics with a particle size in the nano-size range [57]. In another investigation, Liang et al. [55] used a high-temperature solid-state reaction with Ca–Zr–Si oxide-based materials. In that study, the temperature was selected at 1400 °C, followed by sintering for 6 h. However, the ceramic particles in nano cannot be fabricated at this temperature. In 2014, Sadeghpour et al. [39] produced baghdadite powders utilizing a mechanical activation-synthesis technique. They claim this procedure is more straightforward than the sol-gel method to synthesize the baghdadite nanoparticles. Nevertheless, the low amount of gittinsite phase as an impurity detected even at a high sintering temperature (1350 °C). This method generates baghdadite particles with a spherical shape and a mean

crystallite size of less than 50 nm [39]. Another study [30] introduced an efficient surfactant-assisted sol-gel technique to synthesize the bimodal nano-porous baghdadite (utilizing pluronic® (P123) as a surfactant). The specific surface areas vary from 35 to 98 m^2/g. The surface area of the optimal sample and mean pore diameter with 0.025 Pluronic® (P123) were 98 m^2/g and 3.1 nm after sintering at 800 °C for 3 h.

2.3. Mechanical properties of baghdadite ceramic

2.3.1. Bulk form

The sintering process as the main factor in determining the mechanical properties of bulk baghdadite ceramics was considered by Schumacher et al. [38] in 2014. They reported the mechanical properties of pure baghdadite green disk under various sintering schedules. An adjustment of the sintering temperature to 1400 °C and 1450 °C enhanced bending strength to 98 ± 16 MPa and 97 ± 20 MPa, simultaneously. An inverse correlation was identified between flexural strength and porosity in the structure of bulk baghdadite. It was shown that the porosity at 1350 °C (15 ± 4%) was decreased to 0.5 ± 0.8% at 1400 °C. One more influence of raising the sintering temperature was on the fracture toughness of bulk baghdadite, which reported 1.1 ± 0.1 MPa $m^{0.5}$ at 1350 °C and 1.3 ± 0.1 MPa $m^{0.5}$ at 1400 °C [38]. Baghdadite Vickers hardness was measured at 6.1 ± 1.1 GPa at 1350 °C, and it was raised to 7.9 ± 0.2 GPa when sintering was performed at 1400 °C.

2.3.2. Porous scaffold form

In some musculoskeletal applications, the porous baghdadite scaffold would be considered as one of the most useful temporary substrates for growing hard tissues. The ideal synthetic bone scaffold for bone regeneration should be biodegradable, biocompatible and possessing good mechanical properties, a 3D structure with a highly interconnected porous structure [58–60]. Among all the requirements, the mechanical characteristics and architecture of porous scaffolds such as baghdadite ceramic can be affected by various fabrication techniques. Table S1, in supplementary information, shows the physical and mechanical properties of the porous baghdadite ceramic scaffolds prepared by various techniques. It was demonstrated that while the porosity of pure baghdadite fabricated by the freeze-drying method increased from 58.22% to 64.27%, the mechanical strength dropped from 2.1 MPa to 1.3 MPa [39]. In another study [11], the polymer replicate technique was used to produce the porous baghdadite. In wet conditions, the compressive strength and modulus were 0.27 and 15.3 MPa, respectively [11]. Fabrication of a highly porous baghdadite scaffold utilizing the space holder method led to compressive strength and modulus values of 0.52 and 121.5 MPa, respectively, only by sintering at 1350 °C for 3 h [8]. Also, Sadeghzade et al. [8] reported a significant increase in the wet compressive strength of the baghdadite scaffolds after 21 days of immersion in SBF (0.61 ± 0.5 MPa), which is due to the formation and penetration of apatite into the holes of the scaffolds [8]. To facilitate load transmission and minimize stress shielding, the elastic modulus of scaffolds should be analogous to that of the bone tissue to reduce its resorption and degradation [22]. Due to significant modulus mismatch, the tissue becomes stress shielded, which is undesirable because healthy tissue, like bone, must be subjected to tensile forces. Based on the results, the baghdadite modulus in the form of scaffold and bulk can meet the lower end of the reported range for trabecular (0.12–1.1 GPa) and cortical bone (11.5–17 GPa).

2.4. Microstructure and physical properties of pure baghdadite ceramic fabricated by various techniques

2.4.1. Bulk form

The optimal baghdadite ceramic must be dense (pore-free) and single-phase to have high physical and mechanical properties. The physical, biological, and mechanical properties of bioceramics like baghdadite will be heavily influenced by sintering parameters such as temperature,

holding time in a furnace, and heating and cooling rates as pressed [61]. The schematic of the pressing method is shown in Fig. 1B. Evaluation of the microstructure of pure $Ca_3ZrSi_2O_9$ samples demonstrated that boosting the sintering temperature to 1400 °C (Fig. 1B) resulted in a more compact structure and a closer real density to the theoretical one with a smoother and more uniform microstructure. However, grain growth was observed due to increased temperatures [38]. Generally speaking, the smaller the grain size, the stronger and denser the ceramic structure is. Based on various applications for ceramic materials, these materials can be either less or more porous. Depending on the fabrication and sintering process, the properties of the baghdadite can often be closely tailored to the desired application.

2.4.2. Porous scaffold form

Since natural bone includes a porous structure with internal voids known as pores, the design of porous ceramic scaffolds is considered one of the most critical implants for tissue engineering applications [62,63]. The high surface area of scaffolds allows them to interact with cells and the surrounding tissue. Furthermore, this structure allows the exchange of oxygen and nutrients, waste products, the ingrowth of bone tissue, and vascular into the pores. Also, it is worth mentioning that smaller pores lead to hypoxia that prevents vasculature invasion, thus causing chondrogenesis. In contrast, larger pores cause excessive oxygen tension that causes osteogenesis. Therefore, the pore size of scaffolds and interconnectivity must be optimized to make them clinically helpful [52]. It is generally accepted that a bone scaffold should have an interconnected porous network (the porous percentage≥85%) with micro and macro porosity (10–500 μm) to provide the necessary in vivo conditions for bone formation and vascularization. As expected and mentioned before, by increasing the porosity, the mechanical properties of scaffolds will be reduced [63–66]. Various methods have been utilized to fabricate the 3D porous ceramic scaffold, including conventional and developed techniques such as polymer sponge, freeze-drying, space holder method, and 3D printing [67,68]. Nevertheless, the only method that can control the architecture, porosity, shape, size, and interconnectivity of scaffolds is 3D printing. The results show that scaffold fabrication methods significantly affect the critical characteristics of porous implants, which are necessary for implanting them in the human body, including the pore architecture (size, interconnection, open pores, porosity), mechanical, and physical properties. The conventional methods for fabrication of the baghdadite scaffolds, which have been utilized so far, are shown in Fig. 1C–E. For example, Roohani esfahani et al. [11] used the polymer sponge method to fabricate the baghdadite scaffold. The polyurethane as a sacrificial template is soaked into the ceramic slurry, followed by subsequent sintering in the furnace (Fig. 1C). However, this method is not reproducible. Furthermore, the compressive strength of the scaffold produced by this method is insufficient to be used on load-bearing places in the body. According to this method, porous baghdadite with 88% total porosity can be fabricated with 100% interconnectivity, with diameters in the range of 400–500 μm. The baghdadite scaffold promotes the permeability of nutrition and oxygen to target tissue because of its large and interconnected pores. However, the smallest pore size by this method in a porous baghdadite scaffold is limited to roughly 100 μm (Fig. 1C).

Baghdadite particles are compacted with a spacer and then sintered in the space holder method. In this method, incomplete elimination of the space holder agent might lead to cytotoxicity. Pore size and morphology are determined by the morphology of the spacer, while the spacer size and compaction pressure define the properties of the scaffold [8]. Therefore, considering the spacer size and amount can balance the properties of the yield product. For instance, fabricating a baghdadite scaffold using NaCl as a spacer leads to different porosities and compressive strengths in each sample [62]. In the freeze-drying method, the baghdadite scaffold is formed by freezing directly. Ice crystals form columnar porous structures instead of sacrificial polymer foam [62]. Sublimation and temperature combine to form oriented ice crystals. Despite its benefits, the method is not without disadvantages, including

higher energy consumption and long processing times [69].

Since a critical and large bone defect requires more nutrients and oxygen, insufficient porosity and interconnectivity disrupt cell mobility and metabolism. Pores play an important role in bone tissue formation by regulating proliferation, migration, and vascularization [63]. Moreover, the porous surface of the scaffold facilitates mechanical interlock between the inserted scaffold and surrounding bone tissue, resulting in better biomechanical stability at the interface of the scaffold and bone [70].

In comparison to the polymer sponge method, less interconnectivity between the pores can be observed in SEM micrographs of baghdadite scaffolds fabricated by space holder (Fig. 1D) and freeze-drying methods (Fig. 1E) [8,39]. These approaches make it impossible to create porous structures predominantly with open pores [8,11,39,71].

For medical use, compared with the traditional fabrication process, 3D printing technology has the advantage of being able to precisely control the structure of bioceramic scaffold from microscopic to macroscopic scales [72]. This feature allows 3D printing technology to be tailored to the actual needs of patients for defective tissue repair, thus enabling precise medical treatment [73]. The most commonly used 3D printing technologies for biomedical ceramics are inkjet 3D printing, selective laser sintering, direct ink writing 3D, and stereolithography [74]. Fig. 2A–D summarizes the principles, advantages, and disadvantages of these 3D printing technologies.

Among all these 3D printing technologies, the stereolithography technique (SLA, Fig. 2D) can print a 3D baghdadite scaffold layer by layer through photosensitive resin polymerization. Furthermore, photopolymerization allows SLA to print the ceramic scaffold-like baghdadite with high accuracy compared to other techniques and then the customized tissues can be created on demand [75,76]. Standard techniques like polymer sponges and freeze-drying make it challenging to accomplish this level of control in fabricating a baghdadite scaffold. For example, Lu et al. [77] produced the baghdadite scaffold using photolithography. In order to achieve this goal, they combined baghdadite powders with poly (ethylene glycol) diacrylate (50 wt%), a photosensitive resin (40 wt%), and a dispersion (TWEEN 20, and 10 wt%). Two-stage sintering was employed to sinter the printed baghdadite scaffolds (Table S1). In that study, the scaffolds were adjusted to have 50% porosity with a pore size of 500 μm. Fig. S1 (supplementary information) shows the main results and tests performed in that study. As shown in Fig. S1A, they used the early and late passage of HOBs cells, the replicative senescence phenotype, and aged rats for in vitro and in vivo studies. Generally, in that study, it was demonstrated that baghdadite scaffolds provide an anti-senescent microenvironment that directly prevents the induction of cellular senescence in late passaged P7 HOBs and modulates the secretory profiles of P7 HOBs, thereby denying the pro-senescent effects of the secretomes of P7 HOBs. Moreover, baghdadite partially corrected dysfunctional mitochondrial function in P7 HOBs. Baghdadite scaffolds significantly improved the regeneration ability of critical-sized bone lesions in aged rats in vivo. Based on the author's claim, their treatments promote bone regeneration without senolytic drugs. For a more detailed discussion of this study, see section SI.1 and Fig. S1 in Supplementary information.

In another study Mirkhalaf et al. [78] introduced a printing method to design customizable anatomically shaped and sized baghdadite scaffolds. Fig. 3 shows the fabrication and design of baghdadite scaffolds by stereolithography technology and a CAD model with rotated cubic architecture. In that study, baghdadite scaffolds were designed to stimulate bone growth and enhance regeneration in an experimental rat model of heterotopic ossification by combining bone morphogenetic protein-2 (BMP-2, 0, 2, 5, 10 μg) with zoledronic acid (ZA, 2 μg) as a coating. The resin comprised 65 wt% baghdadite particles with a mean particle size of 9.52 μm, 17.5 wt% commercial photopolymers (clear resin V4, Formlabs), and 17.5 wt% dispersion. For printing the baghdadite scaffold, printing settings significantly influence mechanical properties and physical characteristics. For example, baghdadite particle size or

concentration with a thick paste cannot be printed. The wrong particle size or lower concentrations (<65 wt%) of baghdadite particles can result in poor mechanical characteristics after sintering.

Using rotated cubic architecture to manage the stiffness of the baghdadite scaffolds (Fig. 3A) for in vivo testing, results in a reduction in stiffness, which is desired and reduces the possibility of stress shielding. That study showed baghdadite printing potential to develop scaffolds with complex anatomical shapes to repair segmental defects in the human mandible and femur (Fig. 3B).

Such scaffolds can treat deformities caused by accidents, sports events, neonatal trauma, congenital malformations, or diseases like cancer. It has been shown that the volume of bone scaffolds and mechanical characteristics increase with BMP2 dosage. In addition, a significant increase in stiffness and strength was reported when ZA combined with BMP2. For example, combining 2 μg ZA with 10 μg of BMP2 significantly enhanced stiffness and strength compared with controls (two times more than 10 μg of BMP2). Releasing BMP2 and ZA simultaneously induced significant bone ingrowth (Fig. 3C), and increasing the flexibility of the baghdadite scaffold that did not lose its load-carrying capacity substantially at stresses above 8%. Printed bone scaffolds have significant challenges, including the interior structure, which plays a crucial role in curing critical-size defects. In another study [79], they designed a systematic strategy to print five baghdadite scaffolds with different concave and convex surface features, pore interconnectivity, and permeability.

In contrast, the porosity of all scaffolds was 50–54%, with an average pore size of 504–518 μm. They investigated the impact of architecture on bioactivity and the mechanics of baghdadite scaffolds. Fig. 4 shows the architecture of designed baghdadite scaffolds, histology, μ-CT images, and bone volume results. According to their findings, only the pore interconnectivity in 3D scaffolds significantly affected bone tissue regeneration ability (Fig. 4A). It was found that the larger the deviation of pore size distribution, the smaller the new bone volume. They suggested that it is possible to utilize the pore size distribution to predict the tissue regeneration ability of various scaffolds, irrespective of the material type and the design.

Furthermore, a theoretical framework for predicting maximal permeability inside a 3D scaffold may be used to determine the pore interconnectivity of scaffolds and tissue regeneration capability based on the number of permeable pathways per unit volume. Based on the results, the "A" model was the weakest architecture in pre-implantation. In contrast, the "B" and "C" models were 60% stronger than the "A" (Fig. 4E). The finite element analysis (FEA) showed that the increased strength of the architecture "B" and "C" models is attributed to their internal topologies, which reduce internal stresses compared to the architecture "A" model. Furthermore, the scaffold architecture "B" and "C" models that were the stiffest and strongest pre-implantation remained the stiffest and strongest post-implantation.

2.5. In vitro bioactivity and biological properties of pure baghdadite ceramic

2.5.1. Bioactivity of pure baghdadite ceramic

Baghdadite ceramic is the first type of Ca–Zr–Si ceramic system that demonstrates apatite formation ability and is classified as a bioactive ceramic. The crucial biological characteristic of baghdadite ceramic is its potential to support the adhesion, growth, and differentiation of osteoblasts, osteoclasts, and endothelial cells. There is no report of unfavorable or toxic consequences due to incorporating Zr into the Ca–Si system [57]. Wollastonite is used to compare the bioactivity characteristics of new ceramics such as baghdadite [80]. For the first time, wollastonite and baghdadite ceramics were compared in SBF by Ramaswamy et al. [57]. By soaking baghdadite ceramic disks in SBF for seven days, nano/micro-size apatite crystals nucleated (apatite size = 6.8 ± 0.766 mm), causing an increase in baghdadite surface roughness as compared to wollastonite (2.3 ± 0.926 mm) disks [57]. Fig. 5 shows the formation

A **Ink Jetting Technology**

room temperature
nozzle

Advantages
- Low cost
- Suitable for a wide range of bioceramic
- Absence of extra supporting
- Possibility of hardening in room temperature

Disadvantages
- Low mechanical properties
- Rough surface
- Poor printing accuracy
- Entrapment of unbonded powder
- Difficult post processing

sintering
ceramic particles
binder
droplet jetting
powder bed

B **Selective Laser Sintering Technology**

laser

Advantages
- Suitable for a wide range of bioceramic
- No support materials is required
- No organic binder is required
- Good mechanical properties
- Less unbound powder in comparison to ink jetting printing

Disadvantages
- Low surface quality
- High cost
- Low accuracy
- Long time printing processes

sintering
ceramic particles
powder bed

C **Direct Ink Writing Technology**

ink barrel
air pressure
nozzle

Advantages
- Low cost
- Simple method
- Good printing accuracy
- Fast printing method
- Suitable for a wide range of bioceramic
- No entrapment of powder in pores

Disadvantages
- Low accuracy
- Extra support is needed
- Collapse during printing

continuous filament writing
bed
colloidal ink

D **Stereolithography Technology**

build platform
resin tank

Advantages
- High accuracy
- Ability to print complex structures
- High surface quality

Disadvantages
- Expensive
- Extra support is needed
- Collapse during printing
- Slow printing method
- Not applicable for a wide range of materials
- Toxic uncured resin
- Extensive post processing

UV laser
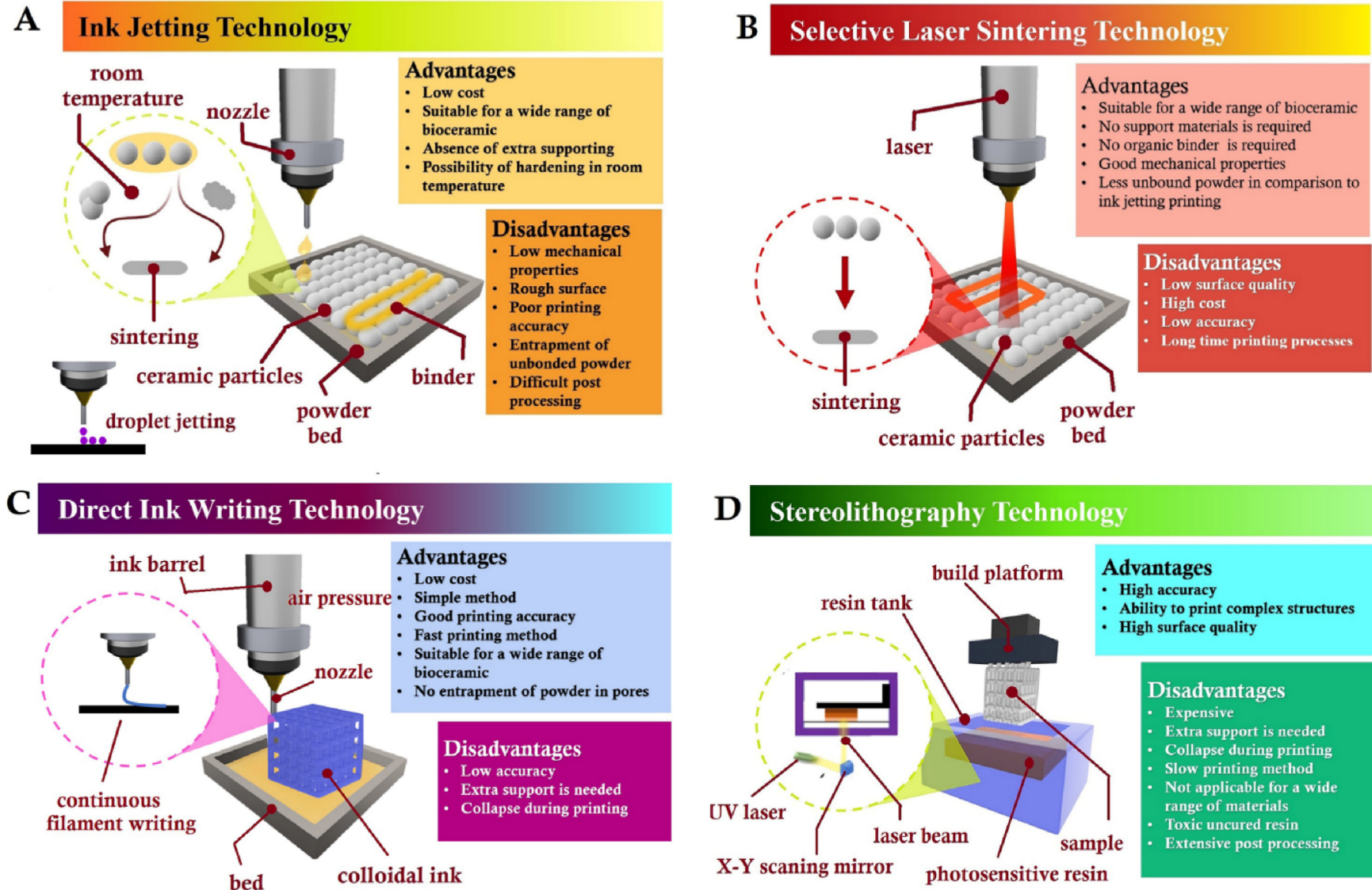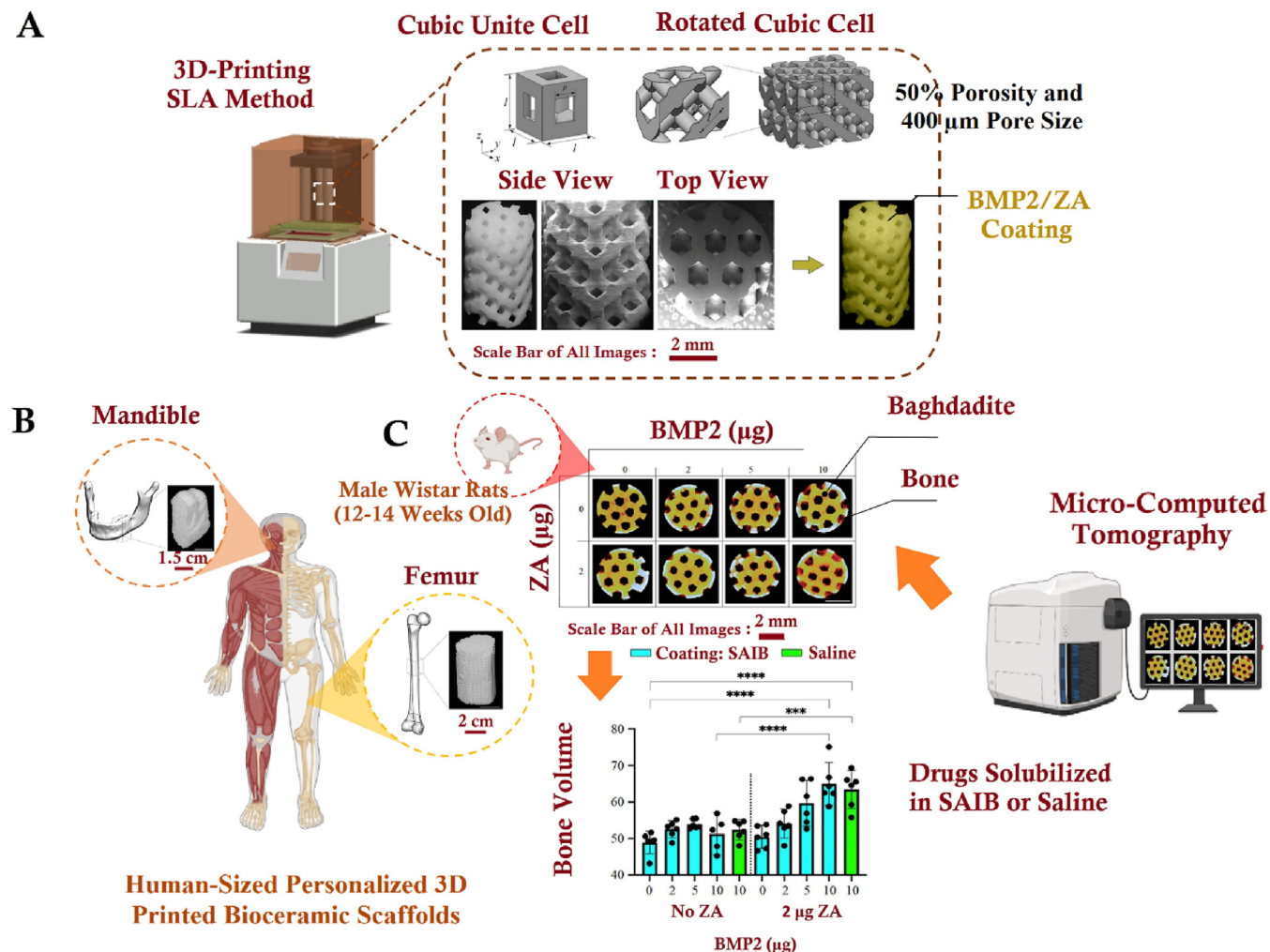X-Y scanning mirror
laser beam
photosensitive resin
sample

Fig. 2. Schematic representation of recognized additive manufacturing methods for printing bioceramics objects and their pros and cons, including (A) ink jetting technology, (B) selective laser sintering, (C) direct-ink writing, and (D) stereolithography.

Fig. 3. (A) Fabrication of baghdadite scaffold by stereolithography method, cubic unit cell by various architecture, optical and SEM photograph of the fabricated baghdadite scaffold, and subsequent coating with BMP2/ZA, reproduced with permission from Ref. [78], (B) human-sized custom made 3D printed baghdadite scaffold for reconstructing mandible and femur, (C) μ-CT results of SAIB (sucrose acetate isobutyrate)- and saline-coated scaffolds with different amounts of BMP2/ZA, μ-CT data of the scaffolds functionalized by different amounts of BMP2/ZA, reproduced with permission from Ref. [78].

mechanism of apatite on the surface of baghdadite ceramic. Even though the pH value of baghdadite in SBF (Ca and Si ions released into the environment) was substantially lower than wollastonite, the formation mechanism of apatite on baghdadite is the same as wollastonite (Fig. 5) [57]. In another study, Sadeghpour et al. reported that the apatite nuclei on the surface of baghdadite scaffolds were not detected until three days after soaking in SBF [39]. In a study published by Liang et al. [55], the degradation rate of plasma-sprayed baghdadite coating under Tris-HCl buffer was investigated. The high release rates for Ca, and Si were detected in the Tris–HCl solution for the baghdadite coating. Based on the literature, baghdadite exhibited weight loss (~9 wt% after 7 days) but only slightly increased the surrounding pH to 7.5–8.0 [71].

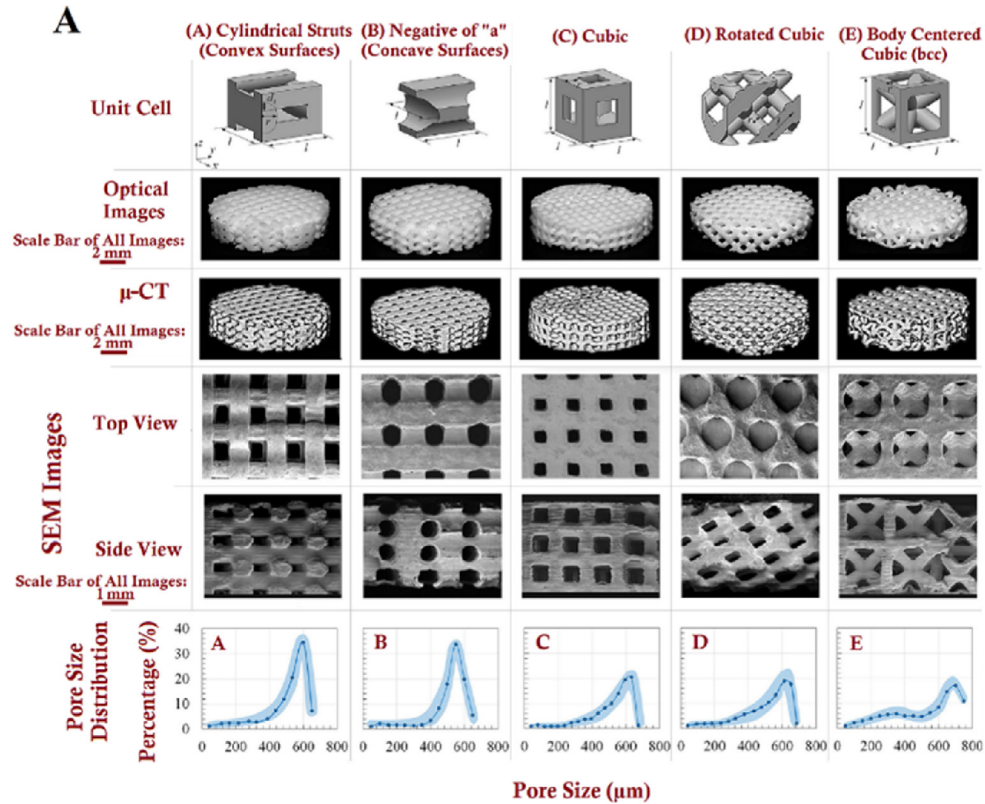### 2.5.2. Biocompatibility and cell friendly characteristics of pure baghdadite ceramic

Table 1 shows the in vitro studies using various cell types and in vivo biological studies, bone formation ability, and histology results of pure baghdadite ceramic in different animals [31,35,55].

Human osteoblast-like cells (HOBs), human osteoclasts (OC), human

endothelial cells (HMEC-1) [57], human adipose-derived stem cells (ASCs) [81], human periodontal ligament cells (PDLSC) [82], human monocytes (differentiated into macrophages) [83,85], and human mesenchymal bone marrow stem cells (hMSCs) [50] have been used to investigate the effects of baghdadite ceramic on various types of cell adhesion, proliferation, gene expression, and differentiation. Fig. S2 in supplementary information shows the interaction between the osteoblast, osteoclast, and endothelial cells with baghdadite and CaSiO₃. The highlights of this study are summarized in Table 1. The cytoskeleton arrangement of human osteoblast-like cells indicates that baghdadite disks produced significantly better adhesion and cell spreading than pseudowollastonite disks (Figs. S2D–E). According to the results, the human osteoblast-like cells stained with rhodamine-phalloidin showed almost clearly defined stress fibers and actin microfilaments immediately after 24 h of culture, compared to the poorly defined actin filament network on the surface of pseudowollastonite disks [57].

Increasing HOBs proliferation, ALP, and osteoblast-related mRNA levels are the main superiorities of baghdadite compared to CaSiO₃. It was found that the proliferation associated with the alkaline phosphatase
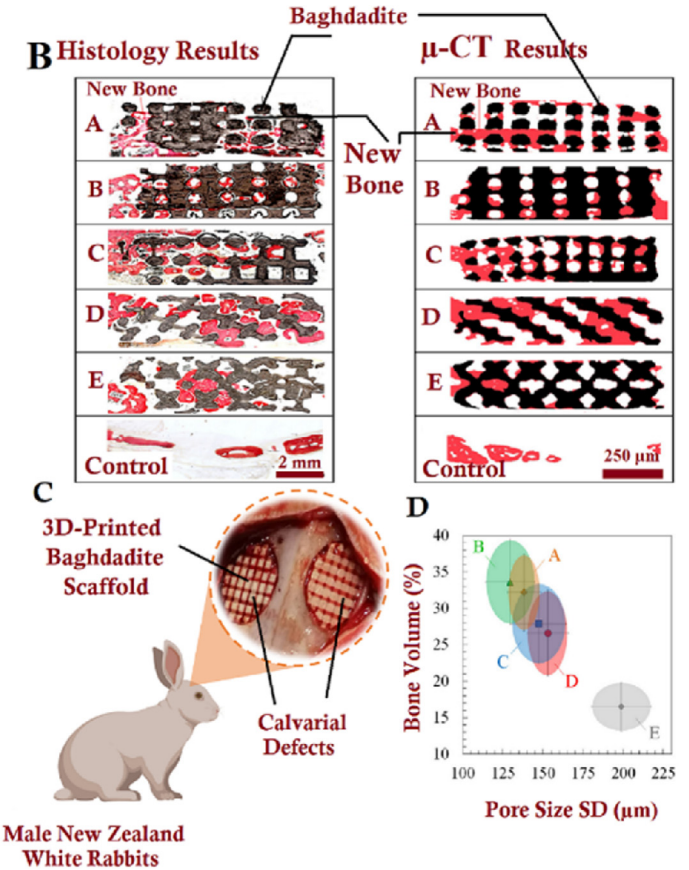
Fig. 4. (A) The geometry of baghdadite scaffolds with various architectures and pore distribution, reproduced with permission from Ref. [79], (B) the histology and μ-CT results for all of the scaffolds with various architectures, reproduced with permission from Ref. [79], (C) schematic representation of baghdadite scaffold implanted in rabbit calvarial defects, and (D) bone volume and pore connectivity as a function of pore size standard deviation, reproduced with permission from Ref. [79].
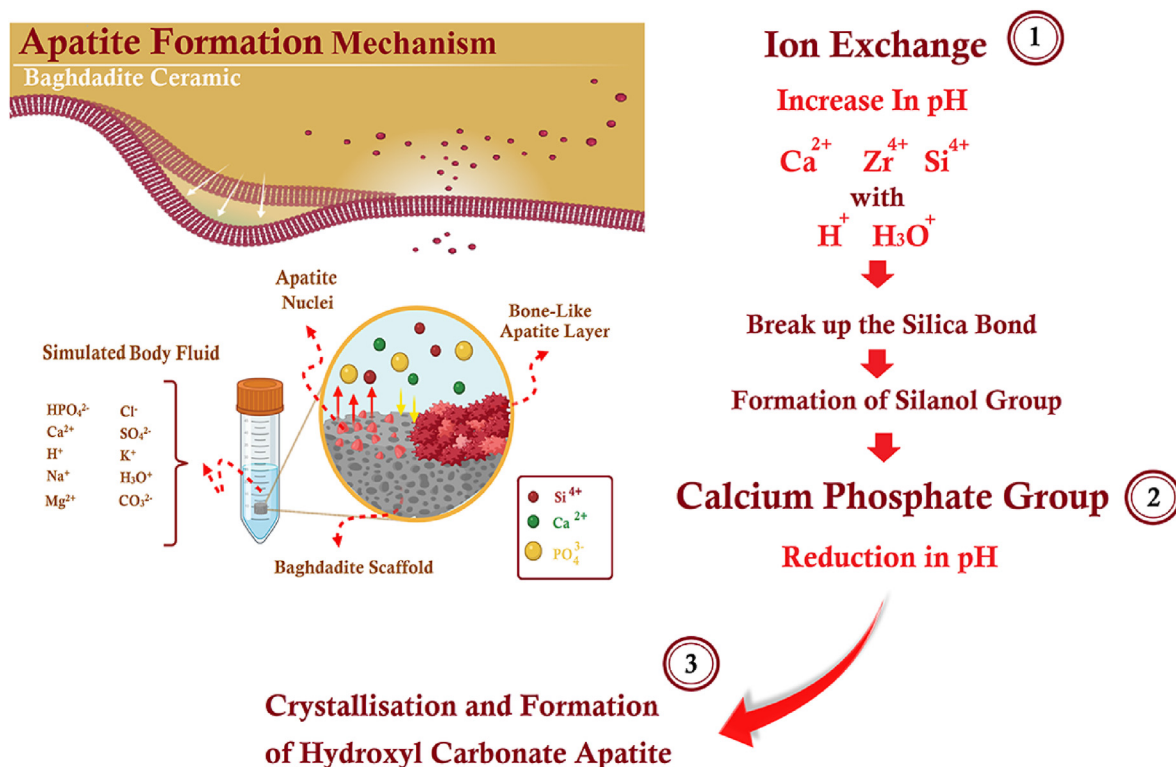
Fig. 5. Apatite formation mechanism on the surface of baghdadite ceramic.

activity of HOBs was dramatically boosted on baghdadite on day 7. Also, mRNA levels of alkaline phosphate were comparable to the pattern with ALP on baghdadite [57]. The expression of collagen type I on baghdadite decreased with time, showing that proliferation was downregulated and osteogenic phenotypes developed. Many factors affect the HOBs proliferation and differentiation, including compositional changes, the dissolution of ions, the pH of the medium culture, and surface roughness (greater surface roughness promotes proliferation and differentiation). A ceramic surface may affect cellular response and activity. The controllable release of Si and Ca ions by baghdadite is found to have a significant role in encouraging the proliferation and differentiation of the HOBs. Variation in the pH value influences osteoblast metabolism as well as gene expression, which was substantially different for the baghdadite (pH = 7.82) and pesedowollastonite samples (pH = 8.1) [57].

The osteoclasts seeded on baghdadite demonstrated that when monocytes are combined, giant cells with filopodia-like morphology and delicate dorsal microvilli are produced at day 21 (Figs. S2F–G). In addition, they found that cells exposed to baghdadite ceramic exhibited a thicker and multinucleated band of filamentous actin (F-actin) compared to cells exposed to pesedowollastonite disks. A combination of some factors, including the expression of protein translation, the localization of $\alpha v \beta 3$, mRNA, actin ring, receptor activator of nuclear factor-$\kappa\beta$ ligand (RANKL), significantly increasing congenital adrenal hyperplasia (CAH II), and an increased expression of cardiothoracic ratio (CTR), has demonstrated the capability of baghdadite to support osteoclast differentiation, spreading, and proliferation [57].

Moreover, human microvascular endothelial cell line (HMEC-1) could stick to, disseminate, and form pseudopodia and microvilli on baghdadite ceramics. There were no characteristic features of the HMEC-1 on $CaSiO_3$. In addition, baghdadite ceramics might promote the growth and survival of endothelial cells by generating well-living conditions for the zonula occludens (ZO-1) protein. Therefore, baghdadite ceramics preserved endothelial cells with typical morphology and the related HMEC-1markers expression, such as zonula occlude (ZO-1) and vascular endothelial cadherin (VE-Cadherin) (Fig. S2J, Table 1) [57].

In another study [81], the human adipose tissue-derived stem cells (ASCs) was used to improve the RUNX2 and osteopontin genes on a baghdadite scaffold in comparison to HA/TCP scaffolds (Table 1). Baghdadite scaffolds did not significantly increase the expression of bone sialoprotein and osteocalcin. When ASCs were seeded on baghdadite scaffold, bone morphogenetic protein (BMP2) expression was increased, and noggin (added to the co-culture media) inhibited the baghdadite scaffold-modulated adipose stem/osteoblast cell crosstalk compared to HA/TCP scaffolds. Therefore, baghdadite scaffolds promote the osteogenic differentiation of ASCs and the crosstalk between ASCs and HOBs (by up-regulating bone morphogenetic protein expression and contributing to their osteogenic differentiation (Table 1)).

Furthermore, baghdadite supports PDLSC adhesion, proliferation, and considerably enhanced cementogenic and osteogenic marker expression of a cementoblastoma-derived protein (CEMP1), catabolite activator protein (CAP), osteopontin (OPN), Wnt/-catenin-related genes of AXIN2 (protein-coding gene), and catenin $\beta 1$ (CTNNB) expression of PDLSC. Si, Ca, and Zr-containing ionic compounds from this ceramic may trigger cementogenic/osteogenic related gene expression of human periodontal ligament cells through stimulation of the Wnt/-catenin signalling pathway. So, it is confirmed that baghdadite can be utilized for periodontal tissue repair (Table 1) [82].

2.6. In vivo biological properties of pure baghdadite ceramic

Some studies have examined the in vivo properties of baghdadite ceramic. Fig. S3 in supplementary information compares the new bone formation ability of the baghdadite in the form of scaffold and sphere. Luo et al. [56] produced baghdadite ceramic spheres using alginate cross-linked by $CaCl_2$ and demonstrated in vivo characteristics of these spheres. After implanting baghdadite spheres for 2 and 4 weeks, bridges were formed between baghdadite spheres at a two-week time point within defects (more mature bone to narrow the defect happened at 4 weeks). Bone growth was found to be more active in the baghdadite ceramic spheres. Also, the dynamic endochondral ossification occurred at

Table 1

Summary of in vitro results using a range of cell types and in vivo biological studies, bone formation ability, and histology results of pure baghdadite ceramic in various animals.

In vitro results							
Cell type	Cell attachment	Proliferation and differentiation	Alkaline phosphatase activity (ALP)	Expression of cell related genes	Cell morphology	Indirect results	Ref.
Human osteoblast like cells (HOBs)	Higher in comparison to CaSiO₃	Higher in comparison to CaSiO₃	Higher in comparison to CaSiO₃	High mRNA expression, bone sialoprotein, and osteoprotegerin	Sheet-like layer	High bioactivity, lower Ca and Si concentration and pH values in comparison to CaSiO₃	[57]
Human osteoclast cells (OC)	Higher in comparison to CaSiO₃	Higher in comparison to CaSiO₃	-	High cathepsin K, carbonic anhydrase II, matrix metalloproteinase-9, receptor	Multinucleated giant cells with filopodia, and fine dorsal microvilli.	Increasing expression of CAH II enzyme in comparison to CaSiO₃	[57]
Human endothelial cells (HMEC-1)	Moderate	-	-	Ability of permeability properties (based on ZO-1 protein detection), increase the mRNA (VE-cadherin), expression of endothelial cells-specific markers such as ZO-1 and VE-cadherin	Normal morphological structure	Well spreading HMEC-1 cells in comparison to CaSiO₃ (no HMEC-1 cells spreading was found on this ceramic)	[57]
Human adipose tissue-derived stem cells (ASCs) + (HOBs)	Higher in comparison to HA/TCP	Higher in comparison to HA/TCP	-	Higher RUNX2, osteopontin, bone sialoprotein and osteocalcin, BMP-2 protein in the presence of noggin, in comparison to HA/TCP	-	Co-culturing of ASCs with osteoblast: enhancing gene expression of RUNX2 and osteopontin in ASCs, co-culturing ASCs with osteoblast: reduced their biological properties in comparison to just culture osteoblast	[81]
Human periodontal ligament cells	Higher in comparison to β-TCP	Higher in comparison to β-TCP	Higher in comparison to β-TCP	Higher CEMP1, CAP, osteopontin, genes in comparison to β-TCP	-	Positive effect of Ca and Si on differentiation of periodontal ligament cells via extracellular signal-released kinases signaling pathway in comparison to β-TCP	[82]
Human monocytes	Higher in comparison to HA/TCP	Cells differentiation to macrophage phenotypes	-	High potential to modulate macrophage behavior in comparison to HA/TCP	-	Maximize bone repair by recapitulating the proper M1-to-M2 transition, higher levels of expression of M2c-related genes in comparison to HA/TCP	[83]
Human mesenchymal bone marrow stem cells	Higher in comparison to control sample	-	Enhancing ALP after 7 and 14 days	-	-	No cytotoxicity, enhancing viability and growth of cells, releasing Ca²⁺ ions	[50]
MG63 cells	Higher in comparison to HA	Higher in comparison to HA	-	-	Presence of filopodia on the surface	-	[18]
In vivo							
Animal model		**Implant Morphology**	**Implantation Period**	**Highlights**			**Ref.**
Wistar rat (8-weeks old)		Spheres	2 and 4 weeks	High bone formation, progression of fibrous ossification in the center of defect region, presence of type I collagen, greater staining intensity of osteopontin in comparison to β-TCP and diopside			[56]
Rabbit (20-weeks old)		Scaffold	12 weeks	High bone ingrowth, bone quality, and implant integration after 12 weeks of healing, extensive new bone formation with complete bridging of the radial defect in comparison to HA/TCP			[11]
Ovine model		Scaffold	26 weeks	Inducing extensive bone formation directly about the implant surfaces with no evidence of chronic inflammation or fibrous capsule formation, bone remodeling by slow in vivo degradation around and within the implant, supporting the long-term repair of large bone defects			[84]
Young (8-weeks old) and aged (18-weeks old) rats		Scaffold	8 weeks	Enhancing bone regenerative capacity of critical-sized bone defects in aged rats in comparison to HA/TCP.			[77]

Abbreviations: Col1: Collagen type 1; OPN: Osteopontin; ALP: Alkaline phosphatase; β-TCP: β-tricalcium phosphate; BMP2: Bone morphogenetic protein; RUNX2: Runt-related transcription factor 2; mRNA: Messenger ribonucleic acid; HA: Hydroxyapatite.

the periphery of the defect within the baghdadite sphere. Based on the results, baghdadite spheres induced more new bone formation compared to diopside and β-TCP.

In addition, an immunohistochemical study revealed that type I collagen stained more frequently in the baghdadite group than in the diopside and β-TCP-sphere groups. Similarly, the higher staining intensity of osteopontin was observed both during the bone regeneration process and the postoperative period in the baghdadite group [56].

In another study, Roohani esfahani et al. [11] implanted a porous baghdadite scaffold with a 4 mm × 4 mm × 15 mm dimension into the large defect in a New Zealand rabbit limb (Fig. S3). According to the radiographical, micro-computed tomography (μ-CT) measurements and histology results, the pure baghdadite scaffold activated bone repair in the radial defects after 12 weeks of implantation. The bone healing

process differed between baghdadite and calcium phosphate composite (Table 1). The baghdadite scaffolds sustained their structural integrity throughout the development of new bone, whereas calcium phosphate scaffolds crumbled [11]. Also, a tight connection of new bone with the surface of the baghdadite ceramic scaffolds (Fig. S3) was observed too. The baghdadite scaffold could be resorbed by osteoclasts and replaced with new bone by osteoblasts before the stability of the material is compromised [86]. Doostmohammadi et al. [87] also obtained the same results by implanting baghdadite nanoparticles in the rabbit tibia. A scaffold can be more effective in forming new bone defects, and the sphere form would be suitable for small bone defects.

Baghdadite scaffolds can interact with bone tissue in a large animal model (the ovine model) without primary cell culture or growth factors. New bone was produced along the baghdadite implant to bind the gap between the scaffold and the implant at a slower rate to fill in the holes. As revealed by clinical evaluations at 3, 12, and 26 weeks, the baghdadite did not cause chronic inflammatory responses in any of those animals. Baghdadite shows this capability that not simply fills the bone defects but should also degrade continuously in vivo [84].

3. Applications of baghdadite ceramic

The selection of biomaterials for bone application is a key step in preparing ideal bone implants. Generally speaking, the selection of bone biomaterials is based on their biocompatibility, biodegradability, bioactivity, and mechanical properties, as well as biological requirements such as being non-toxic and not eliciting inflammatory or immune responses [88]. Though bioceramics seem to fit as biomaterial, the primary drawbacks of bioceramics, including their brittleness, high Young's modulus, and inferior workability, are the vital problems that limit the use of these bioceramics [89,90]. Therefore, composite materials are preferred [91,92]. Biocomposite materials generally possess higher specific strength and modulus than traditional engineering materials. These properties can control the ions released, degradability, pH, and cellular response in static and dynamic environments. Controlling some parameters in those composites means increasing their performance and characteristics. Advanced composites have excellent dynamic and mechanical properties, significant bioactivity, and biocompatibility. In addition, the enhanced biological performance of composite materials allows them to heal injured tissues [93–95]. The biomedical applications of baghdadite composites with other biomaterials are reviewed in the rest of this current study.

3.1. Baghdadite based ceramic matrix composites (CMCs)

Ceramic matrix composites (CMCs) are a subgroup of composite materials. They consist of ceramic fibers, particles, and whiskers embedded in a ceramic matrix. The reinforcement material and the matrix can consist of any ceramic material [96]. Due to the multifold requirements of the materials design for bone regenerative engineering, a composite of baghdadite with other materials has been widely used to combine the advantages of two or more materials to meet these needs. For instance, Khandan et al. [97] created composites for orthopedics and bone regeneration using HA-baghdadite (Table 2). These composites were designed to overcome HA brittleness and poor degradability due to controllable biodegradability and higher strength than HA. Tables 2 and 3 summarized the highlights of studies in the field of the baghdadite-based composite during the 2008–2022 years, including the types of materials, fabrication methods, mechanical and physical properties, in vivo, in vitro, and antibacterial properties.

Despite the perfect biological properties of baghdadite, this ceramic suffers from poor antibacterial properties, resulting in implant infections and post-operative complications. For this purpose, Bakhsheshi-Rad et al. [12] produced scaffolds incorporated with vancomycin antibiotics as a glycopeptide antibiotic active against gram-positive (*S. aureus*) bacteria, effective in the treatment of osteomyelitis. As a result, they observed an

eruption release for 6 h, followed by a steady state release. Furthermore, baghdadite-vancomycin scaffolds presented good antibacterial activity against staphylococcus aureus (*S. aureus*). Also, more attachment and spread of MG63 cells on the baghdadite and baghdadite (1–3 wt.% vancomycin scaffolds compared to the baghdadite 5 wt% vancomycin scaffold (Tables 2 and 3).

Due to some drawbacks of pure baghdadite ceramic, like its brittle inherent, low toughness, low tensile modulus, and lack of resilience, composites of this ceramic have been developed where the base matrix is reinforced with a second phase in the form of particles, whiskers, and fibers. For instance, Sadeghzade et al. [13] developed highly porous diopside (0, 5, 10, 15, 20, and 30 wt%)/baghdadite composite scaffolds using the space holder method with and without polymer coating modification. They reported compressive strength, compressive modulus, porosity, and the pore size of the different scaffolds with various amounts of diopside in the range of 0.28–1.33 MPa, 15.35–155 MPa, 64–78%, and 300–500 μm, respectively. Based on their results, applying polycaprolactone fumarate (PCLF) cross-linked polymer coating on the surface of scaffolds improved their compressive strength and modulus from 1.09 ± 0.1 and 139.3 ± 1.1 to 1.63 ± 0.2 and 189.1 ± 1 MPa, respectively. Furthermore, presence the hydroxyl group (OH) in PCLF polymer has a crucial role in binding the polymer coating to the surface of baghdadite scaffolds and improving its mechanical properties.

3.2. Baghdadite based polymer matrix composites (PMCs)

By incorporating an inorganic phase into a polymeric matrix, new properties can be achieved, such as high strength, flexibility, bioactivity, biodegradability, biocompatibility, and better cellular response in vitro and in vivo [104,106]. The results of some baghdadite-based polymer matrix composites are presented in Table 2. For example, in the No et al. [98], study, baghdadite particles were added to polycaprolactone (PCL) to fabricate an injectable bone void filler. Injections of PCL including 0, 1, 5, and 10 vol% of baghdadite nanoparticles were achievable with relatively modest injection forces (<1500 N) using stainless-steel syringes at 75 °C. The researchers also found that adding 10–30 wt% baghdadite particles into the PCL matrix increases strength and modulus from 36 to 47.1 MPa and 203.8–741 MPa, respectively, compared to pure PCL (31.4 MPa and 205 MPa) (Table 2). Primary human osteoblasts cultured on the PCL-10% Bagh significantly increased osteogenic genes compared to pure PCL (Table 3). In addition, the PCL-10% Bagh showed the maximum flexural strain (29.8 MPa).

Radiopacity is one of the most critical, clinically relevant features that are often overlooked during the design and characterization of implant materials for use as synthetic bone substitutes. The researchers found that PCL can be made much more radiopaque than porous HA by adding >5% vol of baghdadite powder. They noted that zirconium is a transitional metallic element with a high attenuation capacity to X-rays and is routinely used in commercial polymethyl methacrylate (PMMA)-based injectable bone void fillers as a radiopacifying agent [26]. Baghdadite composites exhibit appropriate radiopacity due to the presence of zirconium elements. In other words, the presence of Zr ions in the baghdadite structure provides radiopacity features in the composite. Based on the literature, the X-ray mass attenuation coefficient (μ/ρ, XMAC) of baghdadite and Sr-doped baghdadite were measured at 20.76 and 21.74, respectively, meaningfully higher than cortical bone. This feature is advantageous for medical applications compared to commercial bone replacement materials with XMAC values relatively close to the cortical or spongy bone, like HA, TCP, and bioglass 45S5. In a work published by Karimi et al. [69], They developed artificial porous bone grafts made by 3D printers and freeze-drying (FD) techniques. This research described a novel method for repairing, developing, and proliferating healthy cells in the tumor bone by including stem cells in the polymer matrix and strengthening this composite with baghdadite nanoparticles to increase mechanical and cellular response. Fused deposition modeling (FDM) was initially used to fabricate the shapeless porous scaffold (using

Table 2
Examples of baghdadite based composites reported in the literatures.

Bio-based materials	Matrix	Filler	Method	Types of composites	Application	Compressive strength (MPa)	Compressive modulus (GPa)	Porosity (%)	Ref.
HA/Bagh	HA (10, 20 and 30 wt%)	Bagh	Uniaxially pressed at 90 MPa, subsequent sintering by SPS	CMC	Bone	1.3–2.8	-	49–65	[97]
PCL/Bagh	PCL	Bagh (0, 1, 5, 20, and 30 vol %)	Melting at 75 °C and then extruding	PMC	Injectable material (orthopedic and trauma)	32–46	0.2–0.72	-	[98]
Sr/Bagh	Bagh	Sr (0.7 and 4.8 atom %)-	High temperature solid-state reaction at 1400 °C	CMC	Bone, coating, filler, or scaffold material in non-load bearing applications	-	-	2.8–3.4	[10]
Bagh/PCL/ (nBG)	Bagh	PCL + nBG (coating)	Polymer sponge method (fabrication the baghdadite scaffold) + Dip coating method for modification	-	Bone	0.05–0.52	0.03–0.121	75–85	[11]
Bagh/ Vancomycin	Bagh	Vancomycin (1, 3, and 5 wt%)	Space holder method and subsequent sintering at 1200 °C for 4 h (fabrication the baghdadite scaffold)	-	Bone	0.82	-	80	[12]
HA/Bagh/PCL/ nBG	HA/Bagh	PCL + nBG (coating)	Polymer sponge method (HA/Bagh scaffold) + Dip coating method for modification	-	Bone	-	-	-	[52]
Bagh/DXP/ CN/GX	Bagh	Dexamethasone disodium phosphate/chitosan/gellan-xanthan hydrogel (coating)	Polymer sponge method (baghdadite scaffold) + Dip coating method for modification	-	Bone	-	-	-	[99]
Bagh/PCL/CN/ AZ91	PCL/Chitosan	Bagh	Deep coating method (Nanocomposite Coating on AZ91 magnesium Alloy)	-	Bone	-	-	-	[100, 101]
pMMA/PCL/ Bagh	PMMA/PCL	Bagh (20, 40 and 60 wt%)	Paste creating by ball mill	PMC	Bone cement	70–110	0.4–0.85	-	[102]
Bagh/Dio/ PCLF	Bagh	Dio (5, 10, 15, 20 and 30 wt%)	Space holder method (Bagh/Dio scaffold) + PCLF coating by deep coating method	-	Bone	0.28–1.33	0.015–0.155	63–78	[13]
Bagh/PLLA	PLLA	Bagh coating	Electrospinning of PLLA and immersing plasma-treated mat in baghdadite aqueous solution	PMC	Scaffolds for bone regeneration in critical-sized bone defects	-	-	-	[103]
Brushite/Bagh	Brushite (0, 5, 10, 20, 30, 50, and 100 wt%)	Bagh	Paste creating by ball mill	CMC	Bone cement	7.5–21	0.4–1.4	-	[9]
PCL/Gr/Bagh	PCL	Gr (1 w/v%)/Bagh (1, 3, and 5 w/v %)	Electrospinning	PMC	Bone	1.4–8.3	0.76–4.09	-	[104]
PEI/PSS/Bagh/ Ag	PEI/PSS	Bagh/Ag	Deep coating method	PMC	Bone				[105]
Bagh/PCL	Bagh (30, 40, and 50 wt%)	PCL coating	Polymer sponge method (Bagh scaffold witlzheimeranentrations) + Dip coating method (PCL, various time of soaking (10 and 20 s))	-	Bone	0.18–1.31	-	70–83	[54]
Bagh/PCL/Gr	Bagh	PCL/Gr coating	Polymer sponge method (Bagh scaffold) + Dip coating method (PCL/Gr coating)	-	Bone	-	-	-	[46]
N6/Bagh	N6	Bagh (0, 3, 5, and 10 wt%)	Using Cuttlefish bone as a sacrificial template for fabricating scaffolds	PMC	Bone	0.47–1.41	0.003–0.006	70–91	[106]
	EC-PLA/Alginate			PMC	Bone	0.5–9	-	65–85	[69]

Table 2 (*continued*)

Bio-based materials	Matrix	Filler	Method	Types of composites	Application	Compressive strength (MPa)	Compressive modulus (GPa)	Porosity (%)	Ref.
PLA/Bagh/Alginate/Fe₃O₄		Bagh + Fe3O4(10, 20, and 30 wt%)	Fused deposition modeling (FDM) with the electroconductive filament + freeze-Drying method.	-					[107]
Bagh/CN	Bagh	Chitosan coating	Polymer sponge method (baghdadite scaffold) + dip coating method (chitosan coating)	-	Bone	0.2–4.05	-	60–83	[78]
Bagh/BMP2/ZA	Bagh	BMP2(0, 2, 5, and 10 µg)/ZA (0, and 2 µg) coating	3D-printing method (stereolithography) and deep coating	-	Bone	-	-	-	[47]
Bi/Bagh	Bagh	Bi(0, 0.1, 0.2, and 0.5 wt%)	Solid-state synthesis route and subsequent sintering at 1350 °C for 3 h	CMC	Bone and enhancing radiopaque feature	200–275	3.5–5.6	-	[7]
Bagh/PCL/Gr	Bagh (30 wt%) scaffold	PCL-Gr (0.1, 0.3, and 0.5 wt%) coating	Polymer sponge method (Bagh scaffold) + Dip coating method (PCL/Gr coating)	-	Bone	0.18–3.33	0.007–0.6	68–83	[108]
Zn/Bagh	Bagh	Zn (0, 0.1, 0.25 and 0.5 wt%)	Solid-state ceramic synthesis route and subsequent sintering at 1350 °C for 3 h	CMC	Bone	-	-	-	[109]
Bagh/CN/316L	316L	CN/Bagh (0, 0.5, and 1 wt%)	Electrophoretic deposition	-	Bone	-	-	-	

Abbreviations: HA: hydroxyapatite; Bagh: baghdadite; PCL: polycaprolactone; Sr: strontium; nBG: nano-bio glass; CN: chitosan; PMMA: polymethyl methacrylate; Dio: diopside; PCLF: poly(caprolactone fumarate); PLLA: poly-ʟ-lactic acid; Gr: graphene; PEI: polyethyleneimine; PSS: poly(3,4-ethylenedioxythiophene) polystyrene sulfonates; PLA: polylactic acid; ZA: zoledronic acid; Bi: bismuth; Zn: zinc; Ag: silver; DXP: dexamethasone disodium phosphate; G: gellan; X: xanthan hydrogel; N6: Nylon 6.

electroconductive polylactic acid (PLA) filaments). The printed scaffold was inserted into the alginate-based solution composed of magnetite nanoparticles (MNPs) and 0, 10, 20, and 30 wt% baghdadite nanoparticles. The four samples were then coated using the freeze-drying technique at −45 °C and 0.01 m bar. By assessing the mechanical properties of the scaffolds, the results indicated that they could maintain their mechanical properties in dry conditions and sustain the same mechanical properties as cortical bone, about 6.5 MPa in the case of 20% and 72% porosity. According to biological features such as weight loss and pH changes, the samples did not experience significant dissolution and degradation. Moreover, the rate of bone growth and apoptosis occurred to a greater extent in the sample with the highest baghdadite concentration.

3.3. Baghdadite as substrate + polymer coating composites

Jiao Li et al. [110] evaluated the histology and bone regeneration of baghdadite-polycaprolactone -nano bio-glass (Bagh-PCL-nBG) scaffolds (pure baghdadite scaffolds as the control sample was chosen in this study, Tables 2 and 3). Both unmodified and modified baghdadite scaffolds possess significant bone bridging within the implanted defects without cells or bioactive molecules supporting, high under taking the mechanical stress at the defect site (Tables 2 and 3). In fact, surface modification of baghdadite scaffolds might result in enhanced mechanical performance at load-bearing defect areas during the early stages of healing without affecting the bioactivity of the scaffold. According to the biomechanical data, both groups achieved stiffness values of 10–25% of the undamaged tibia. Based on the histological analysis and micro-computed tomography images, a highly integrated host bone and implants were found at the proximal and distal interfaces. Their findings are in good agreement with the earlier work by Roohani esfahani et al. (implanting these scaffolds in the rabbit) [11].

In another study by Sehgal et al., a modification of the baghdadite scaffold encapsulated chitosan nanoparticles (CN) embedded in a layer of nanostructured gellan and xanthan hydrogel (GX) was reported [99]. Studies of drug release in vitro showed that a hydrogel-coated baghdadite scaffold loaded with dexamethasone disodium phosphate/chitosan/gellan-xanthan hydrogel (DXP–CN–GX) resulted in a sustained release of the pharmaceutical over five days (78% drug release) compared with an abrupt release over just 1 h (92% drug release in just 1 h). Also, it was reported that MG63 cells within dexamethasone disodium phosphate/chitosan/gellan-xanthan hydrogel/baghdadite (DXP–CN–GX–Bagh) scaffolds showed a significant increase in the expression of early and late osteogenic markers of alkaline phosphatase, collagen type I and osteocalcin, which was not observed in the unmodified baghdadite scaffold. The researchers also found that the temperature of the solution, the concentration of polymer, and crosslinkers are the vital factors affecting gelation time. According to Tables 2 and 3, the dexamethasone disodium phosphate/nanostructured hydrogel integrated within the porous baghdadite resulted in the steady state release of dexamethasone disodium phosphate. This composite showed a high potential to improve osteogenic differentiation.

3.4. Bone cements

Combining bioceramics and polymers is essential for fabricating bone cement, which possesses apatite formation, and osteogenesis capability. Pahlevanzade et al. [102] introduced a polymethyl methacrylate (PMMA)–polycaprolactone (PCL) bone cement incorporating baghdadite nanoparticles. This cement demonstrated excellent bioactivity compared to cement without baghdadite. The survival, adhesion, and spreading of MG63 cells were significantly increased following the addition of 20 wt% baghdadite nanoparticles. Furthermore, the polymerization temperature was reduced to 67.3 °C. After implantation, this phenomenon could lead to a reduction in tissue damage. Hence, the cement containing baghdadite provides the synergistic benefits of suitable mechanical properties,

Table 3
In vivo, in vitro, and antibacterial properties of baghdadite based composites reported in the literature.

Bio-Based Materials	In vitro		In vivo		Antibacterial evaluation	Ref.
	Cell type	Highlights	Animal model	Highlights		
PCL/Bagh	Osteoblast cells	PCL-10%Bagh possess good HOBs adhesion, proliferation and differentiation, new bone formation, no apatite formation ability	-	-	-	[98]
Sr/Bagh	Osteoblast cells	Positive effect of Sr on HOBs cellular activity, highest ALP activity on sample with 0.5 wt% Sr after 7 days of culturing, higher cell attachment and differentiation of HOBs compared to baghdadite	-	-	-	[10]
Bagh/PCL/ nBG	-	-	Rabbit (20-weeks old)	New bone formation, no signs of rejection, necrosis, or infection, open spaces within the newly formed bone consistent with the possible recovery of radial architecture through the formation of an endocortical space	-	[11]
Bagh/PCL/ nBG	-	-	Merino wethers	Bagh/PCL/nBG scaffolds induced substantial bridging in the defect and bone infiltration into the scaffold implant in the absence of supplementation with cells or growth factors (over 26 weeks)	-	[110]
Bagh/ Vancomycin	MG63 cells	Cell viability was reduced by increasing the incubation time and vancomycin concentration (up to 5 wt%).	-	-	Inhibition of growth and proliferation of *Staphylococcus aureus*.	[12]
Bagh/DXP/ CN/GX	MG63 cells	Enhancing cell proliferation, ALP activity and higher Ca deposition in CN–GX hydrogels compared to GX hydrogels, no significant difference in proliferation in DXP–CN–GX hydrogels compared to GX hydrogels at day 14 of culture, DXP releasing from the nanoparticulated hydrogel was biologically more active compared to direct loading within the hydrogel.	-	-	-	[99]
Bagh/PLLA	Adipose tissue-derived mesenchymal stem cells (AD-MSCs)	RUNX2 enhanced BMP9, which induces ALP activity, baghdadite and PLLA improved osteogenic differentiation of AD-MSCs by mimicking ECM.	-	-	-	[103]
Bagh/Brushite	Osteoblast cells	Increasing proliferation, and pH compared to unmodified brushite cement, strong reduction in phosphate release, better cytocompatibility of the materials.	-	-	-	[9]
PCL/Gr/Bagh	P19 embryonal carcinoma cells	PCL-1Gr-5Bagh scaffold caused further adhesion, viability, and proliferation of the cells, good proliferation of human fibroblast cells on PCL-1Gr-3Bagh and PCL-1Gr-5Bagh nanocomposite scaffolds	-	-	-	[104]
PEI/PSS/ Bagh/Ag	MC3T3-E1 pre-osteoblast	dramatically upregulating self-assembly of osteo differentiation markers, including ALP, collagen secretion, and Ca deposition by using baghdadite, promoting ALP expression and ECM (osteogenesis) by releasing Ca, Si and Zn ions, catechol and amine groups of PDA and PEI can exert beneficial osteogenic effects by serving as active recruiting sites of mineral ions and aid in apatite nucleation and growth.	-	-	self-antibacterial coating against *Staphylococcus aureus* adhesion	[105]
Bagh/PCL	Saos-2 cells line	No cytotoxicity, good attachment and proliferation of cells on the both coated Bagh and Bagh/PCL scaffolds, less cell viability for scaffold with PCL coating in comparison to uncoated Bagh	-	-	-	[54]

Table 3 (*continued*)

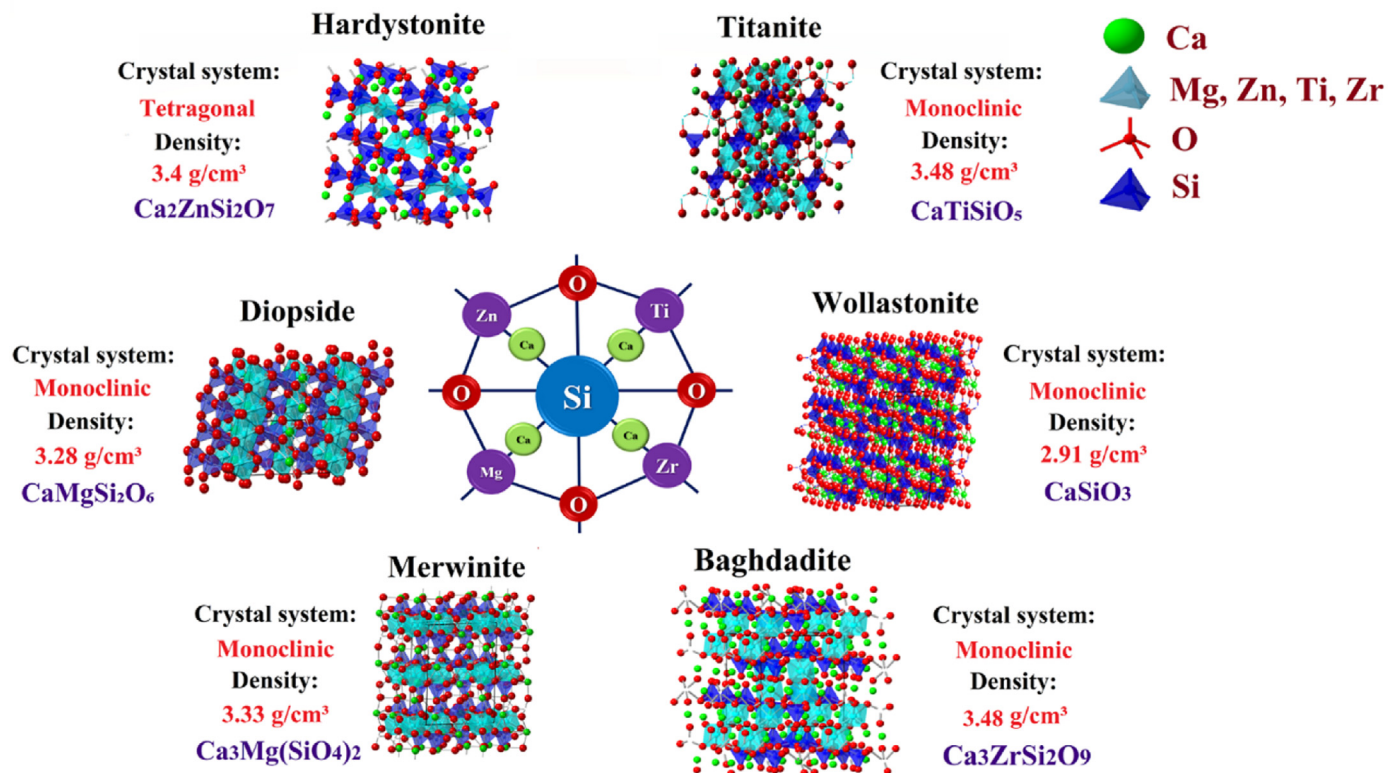| Bio-Based Materials	In vitro		In vivo		Antibacterial evaluation	Ref.
	Cell type	Highlights	Animal model	Highlights		
Bagh/Dio/PCLF	Bone marrow stem cells (BMSc)	Good attachment, high proliferation, and spreading of the BMSc cells on the surface of Bagh/Dio/PCLF scaffold, good biocompatibility, no toxicity	-	-	-	[27]
N6/Bagh	MG63 cells	Increasing cellular activity, and cell viability, better cell attachment and spreading by increasing the amount of Bagh in composite scaffold in comparison to N6	-	-	-	[106]
PLA/Bagh/Alginate/Fe$_3$O$_4$	-	Sample including 20 wt% baghdadite has less toxicity than other samples	-	-	-	[69]
Bagh/CN coating	Human bone marrow mesenchymal stem cells	Enhancing growth, proliferation, adhesion, and viability, activation of Zr ions on the differentiation of cells, bone formation and repair capability	-	-	-	[45]
Bagh/BMP2/ZA	-	-	Wistar rats (12–14 weeks old)	The significant bone formation resulted from co-delivery of BMP2 and ZA capability of BMP2 and BMP2/ZA new bone formation in non-osseous settings; more potent in a critical defect setting as the drugs, enhancing effect in a region with more abundant osteoprogenitors.	-	[78]
Bi/Bagh	Osteoblast cells (HOBs)	Higher HOBs viability, cell attachment efficiency on Bi0.1-Bagh compared to pure Bagh and Bi0.2- Bagh	-	-	-	[47]
Bagh/PCL/Gr	MG63 cells	Bagh, Bagh/PCL, and Bagh/PCL/Gr scaffolds lacked destructive and toxic effects on cells, Gr enhanced cells viability and proliferation (due to higher hydrophilicity),	-	-	-	[7]
Zn/Bagh	MG63 cells	High biocompatibility (hemolysis rate <5%), increasing Zn results in lower hemolyzed blood cells, and reducing the number of cells attached on the surface	-	-	Decreasing viability of *E. coli* and S. Aureus bacteria with increasing zinc oxide addition in calcium zirconium silicate.	[108]

Calcium Silicate Based Ceramics

Fig. 6. Illustration of the crystal structures of some of calcium silicate-based ceramics.

good bioactivity, and favorable cytocompatibility for bone healing in orthopedic implants. Calcium phosphate cement, such as brushite, is a well-known example of biodegradable cement [60,188–190]. Nevertheless, the low radiopacity and acidity of these types of cement limit their applications. To improve these drawbacks of brushite, Young Jung No et al. [9] examined the effects of substituting β-TCP with baghdadite at various concentrations (0, 5, 10, 20, 30, 50, and 100 wt% of β-TCP) on the brushite cement reaction and its physicochemical properties. Their results demonstrated the dissolution of baghdadite during the cement reaction without affecting the crystal structure of the precipitated brushite. As a result of the increased baghdadite incorporation into brushite cement, the radiopacity has increased significantly, with more than 2-fold of the aluminium at 50 wt% baghdadite. Also, the compressive strength of brushite cement increased from 12.9 ± 3.1 MPa to 21.1 ± 4.1 MPa with just 10 wt% baghdadite. The pH of the culture medium approached physiological pH by increasing the baghdadite nanoparticles in the cement (pH $= 6.47$ for pure brushite, pH $= 7.02$ for brushite with 20% baghdadite substitution). Additionally, baghdadite changed the ionic content of the culture medium, which affected the proliferation of primary human osteoblasts in vitro. Given that calcium silicates typically display hydraulic activity and are commonly employed in portland cement, some researchers [9] believe that baghdadite might also contain such hydraulic reactivity and would be able to make self-setting cement. In order to prove this hypothesis, they utilized a mechanical activation method for synthesizing baghdadite cement (selecting various milling times with distilled water). The self-setting of baghdadite occurred without further additives, and baghdadite cement has shown high potential for biomedical use, either in bone replacement or due to the radiopacity feature as an endodontic filler.

3.5. Doping elements in baghdadite ceramic

Specific metal ions with therapeutic effects have been incorporated within bioceramic chemical structures to overcome the disadvantages of new materials and favor their use in different biomedical applications. These metallic ions are essential for multiple metabolic functions and are required to grow, develop, and maintain healthy bones [2,111–113]. Modifying bioceramics' interfacial chemistry, such as baghdadite, with molecules, atoms, and ions is lucrative in bone formation and its biological features like cell interaction in the body [2,112,113]. In a study, baghdadite ceramic was doped with divalent Sr ions due to their beneficial effects on bone mineralization and osteoblast cell contact. The authors suggested that the chemistry of baghdadite ceramic is thus one of the most important aspects influencing the proliferation and differentiation of osteoblast cells [10]. Incorporating various metal ions into the baghdadite structure always leads to complex structures with various bond strengths between ions, which alters ion release. Schumacher et al. [10] also mentioned the enhancement effect of strontium on alkaline phosphatase activity, osteoblast cell attachment, proliferation, and differentiation compared with unmodified baghdadite.

As mentioned before, μ-CT imaging of an implant with a high radiopacity will allow surgeons to visually check the location and status of the implant by providing a significant contrast with the surrounding tissue. In determining the radiopacity of a material, density and elemental composition are the significant factors. Therefore, elemental doping of bioactive ceramics such as baghdadite might beneficially affect their radiopacity and antibacterial activities [47,114,115]. For instance, Jung No et al. [47] doped bismuth ions in baghdadite ceramic to boost its radiopacity capability. They described the impact of integrating bismuth (Bi) ions into the baghdadite crystalline structure ($Bi_xCa_{3-x}ZrSi_2O_9$, x = 0, 0.1, 0.2, 0.5). The energy-dispersive X-ray spectroscopy data shows baghdadite with 0 and 0.1 wt % Bi kept crystalline homogeneity,
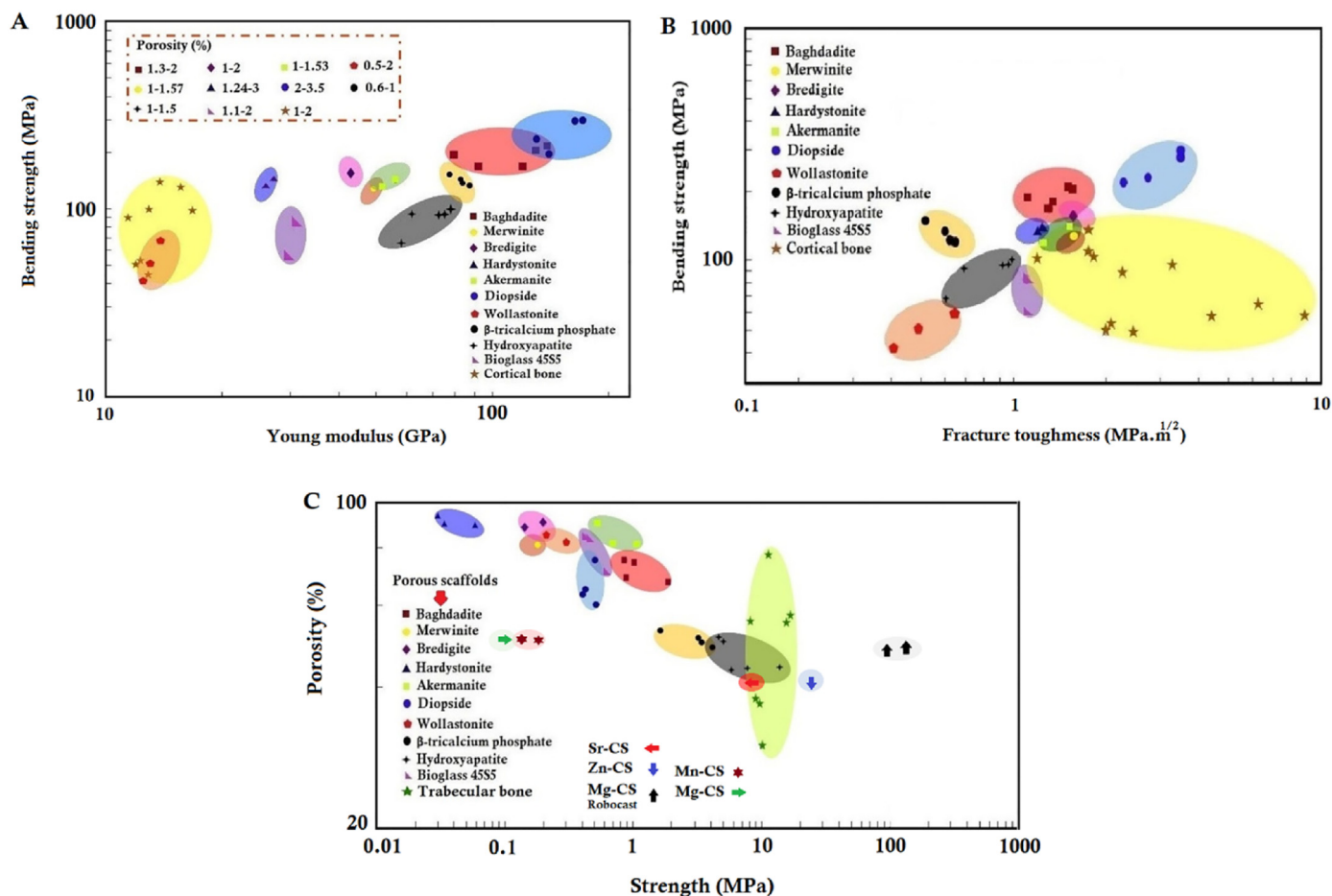
Fig. 7. Mechanical properties of various calcium-silicate-based ceramics in the form of porous and dense, as well as β-tricalcium phosphate (β-TCP), bioglass 45S5, hydroxyapatite, cortical, and trabecular bone, are included for comparison (A) bending strength as a function of Young's modulus, (B) bending strength as a function of fracture toughness, (C) compression strength as a function of porosity (for porous scaffold materials) [12,13,25,26,38,63,128,134–151].

whereas baghdadite with 0.2 wt % Bi developed zirconium-rich crystalline areas. Baghdadite with 0.1 and 0.2 wt % Bi was non-degradable after 56 days of immersion in culture media. No significant pH changes were found in a sample containing 0.1 wt% Bi at day 56. Baghdadite with 0.1 wt% Bi demonstrated comparable strength (200–290 Mpa) and modulus (4–5 GPa) to pure baghdadite and considerably higher compressive strength and modulus than baghdadite with 0.2 wt% Bi (150–200 MPa and 3.5–4 GPa) throughout 56 days of soaking.

The most common infection problem in an orthopedic implant is the adhesion and colonization of bacteria on the surface of the implant or adjacent tissues. However, baghdadite ceramic suffers from low antibacterial capability. Yadav et al. [108] incorporated zinc oxide into the baghdadite ceramic to inhibit bacterial adhesion. Based on their results, the hemolysis rate was observed at a concentration of less than 5 wt% on the baghdadite. Spreading of MG63 cells was found in a large number on the pure baghdadite ceramic compared to 0.5 mol% zinc oxide-baghdadite. It was found that zinc oxide-baghdadite composites were more effective in preventing bacterial growth and were more inactive towards *E. coli*. In this composite, the antibacterial mechanism comes from the generation of hydrogen peroxide and the leaching of zinc (Zn) ions into the media. Although the Zn-substituted baghdadite ceramic has excellent antibacterial properties, the number of cells attached to the surface of this sample decreased with increasing zinc oxide content.

3.6. Coatings

Biomaterial implants such as metals and ceramics can be coated with ceramic or composite coatings made from baghdadite ceramic [54,100, 101]. Liang et al. [55] used baghdadite particles as a plasma-sprayed coating on a Ti–6Al–4V alloy substrate for hard tissue replacement applications. A high cooling rate and the complex structure of baghdadite ceramic resulted in the coating being predominantly made of baghdadite phase with an amorphous form (because it melted fast and was subsequently cooled onto the surface of the platform). Baghdadite coatings with an average roughness Ra = 9.844 ± 1.215 μm and a bond strength of 28 ± 4 MPa showed substantially more excellent characteristics than plasma-sprayed hydroxyapatite coatings reported earlier [116]. In addition, as a result of incorporating zirconium to the crystal structure of baghdadite coatings, they demonstrated significantly higher chemical stability than calcium silicate [117].

Other research examined the in vitro bioactivity, degradation, adhesion, microstructure, roughness, and cytocompatibility of the baghdadite and HA ceramic coatings [118]. The findings indicated that the baghdadite coating on the Ti–6Al–4V substrate had a stable microstructure and more consistent hardness (325.5 ± 55.2 HV) than the HA coating (118.3 ± 21.2 HV) because of the presence of Zr elements in the baghdadite structure. In addition, the surface roughness of the baghdadite coating exhibited less fluctuation than that of the HA coating. The Ra results were 9.9 ± 0.6 μm and 10.1 ± 0.9 μm for baghdadite and HA coatings, respectively. The average hardness and modulus of the baghdadite coating were 8.2 ± 2.9 GPA and 103.2 ± 26.6 GPa under

Table 4
Apatite formation ability, dissolution behavior, pH, in vitro, and in vivo results of calcium-silicate-based ceramics using various morphology.

| Ceramics | Simulated body fluid | | | | In vivo | | | | |
	Apatite formation ability	pH of aqueous media after 7 days	Dissolution behavior	Ref.	Animal model	Type of implants	Implantation period	Highlights	Ref.
Wollastonite	Excellent	8.1–8.6	High	[154]	Rat	Scaffold	6 and 12 weeks	Bone regeneration and maturation, integration of the defect area with the surrounding of normal bone tissue, vascularization after 12 weeks of surgery	[155]
Sr-α-CaSiO₃ (1, 2.5, 5, and 10 wt% Sr)	Excellent for percentage more than 2.5 wt% Sr, Moderate less than 2.5 wt% Sr	8.3–7.8	Moderate	[147]	-	-	-	-	-
Mg–CaSiO₃ (10% Mg) fabricated by robocast method	Mild apatite-like phase transformation	7.7	Moderate	[145]	Rabbit	Scaffold	6–18 weeks	No changes in new bone regeneration rate and lower bone regeneration capability of Mg-β-CaSiO₃ compared to CaSiO₃ scaffold	[145]
Mg–CaSiO₃ (10 wt% Mg) fabricated by polymer sponge method	-	8.6	Moderate (15–20 wt% weight loss after 7 days soaking)	[146]	Rat	Scaffold	4–12 weeks	Increasing new bone formation and maturation compared to CaSiO₃	[146]
Mn–CaSiO₃ (10 wt% Mn) fabricated by polymer sponge method	-	7.7	Moderate (15–20 wt% weight loss after 7 days soaking)	[146]	Rat	Scaffold	4–12 weeks	Increasing new bone formation and maturation compared to CaSiO₃	[146]
Zn-α-CaSiO₃ (1, 3, and 5 wt% Zn), (cell type: MG63)	Higher apatite formation ability compered to CaSiO₃	-	Moderate	[144]	-	-	-	-	-
Akermanite	Moderate	7.4	Moderate	[156]	Rabbit	Scaffold	8–16 weeks	Higher mineral apposition rate which results in enhanced bone regeneration, faster angiogenesis compared to the β-TCP	[157]
Diopside	Moderate	8.1	Moderate	[136]	Rat	Powder	2–4 weeks	Higher bone regeneration, evidence of dynamic endochondral ossification; higher Col1 expression and similar OPN expression compared to β-TCP	[56]
Bredigite	Excellent	7.3	High	[137]	Rabbit	Scaffold	4–12 weeks	Promoting vascularization, bone regeneration, bone marrow cavity reconnection and formation	[158]
Hardystonite	weak	7.2	Very slow	[159]	Wistar rats	Scaffold	6 weeks	Effective support for bone ingrowth into the bone pores, vascularization, and new bone formation capability throughout the implant in comparison to β-TCP	[159]
Baghdadite	Excellent	7.5–8	Moderate	[11]	Rabbit	Scaffold	12 weeks	High bone ingrowth, bone quality, and implant integration after 12 weeks of healing, extensive new bone formation with complete bridging of the radial defect	[11]
Merwinite	Moderate	8.3	Moderate	[160]	Rat	Powder	2–8 weeks	Enhancing osteogenesis, and faster new bone formation in defect compared to HA	[161]

In vitro Ceramics	Cell Proliferation, differentiation and adhesion	Cell morphology	Highlights	Ref.
Wollastonite[a]	Higher compared to β-TCP extract	Irregular morphology, and physical contact with each other	Higher ALP activity compared to β-TCP, observation of apatite formation ability in cell culture media, no apatite on β-TCP surface	[162]
Sr-α-CaSiO₃ (1–10 wt % Sr)[a]	Increasing proliferation compared to CaSiO₃	-	-	[147]

Table 4 (*continued*)

| Ceramics | Simulated body fluid | | | | In vivo | | | | |
	Apatite formation ability	pH of aqueous media after 7 days	Dissolution behavior	Ref.	Animal model	Type of implants	Implantation period	Highlights	Ref.
Mg-β-CaSiO₃ (10% Mg), (cell type: bone marrow stromal cells) fabricated by robocat method	Highest viability of CaSiO₃ compared to that of cells on the TCP and Mg-β-CaSiO₃ scaffolds,				Polygonal and widespread forms, abundant prominent filopodium and unidirectional lamellipodium extensions			Lower ALP activity, no difference in the expression of all the analyzed osteogenic genes, including COL1, OCN, Sp7 and Runx2 compared to CaSiO₃	[145]
Zn-α-CaSiO₃ (1, 3, and 5 wt% Zn)	Enhanced cell viability, and adhesion				Spindle shaped morphology			-	[144]
Mg–CaSiO₃ (10 wt% Mg), (cell type: bone marrow stromal cells) fabricated by polymer sponge method	Toxic environment due to pH higher than 9, lower cell prefiltration compared to TCP, higher expression levels compared to CaSiO₃				Widespread forms, abundant filopodium			Higher expressions of both ALP and Col-I, promoting the osteogenic differentiation of BMSCs compared to CaSiO₃	[146]
Mn–CaSiO₃ (10 wt% Mn), cell type: bone marrow stromal cells), fabricated by polymer sponge method	Toxic environment due to pH higher than 9, lower cell prefiltration compared to TCP, higher expression levels compared to CaSiO₃ but lower compared to Mg doped CaSiO₃				Widespread forms, abundant filopodium			Higher expressions of both ALP and Col-I, promoting the osteogenic differentiation of BMSCs compared to CaSiO₃, but lower compared to Mg doped CaSiO₃	[146]
Akermanite[a]	Good spreading and proliferation (increasing cell viability)				Elongated and flattened appearance after 24 h culturing			No cytotoxic effects, enhanced ALP activity, mineralization, and osteogenic gene expression (ALP, BMP-2, Col1, RUNX2)	[156, 163]
Diopside[a]	Good attachment, high proliferation, and differentiation				Flat layer like			presented a comparable ALP activity with HA scaffolds and tissue culture plates	[136]
Bredigite[a]	Enhanced proliferation by increasing culturing time				Round morphology after 6 h culturing elongated, flattened and minor filopodia morphology after 12 h			Significantly stimulates cell growth within a certain concentration range	[137]
Hardystonite[a]	Supported the in vitro adhesion, growth and differentiation				-			Enhanced ALP activity with increasing with culturing time, hardystonite enhanced expression of alkaline phosphatase, RUNX2, osteopontin, osteocalcin and bone sialoprotein	[159]
Baghdadite[a]	High cell attachment, proliferation and differentiation				Sheet-like layer.			High ALP activity, high mRNA expression and high levels of bone-related genes (collagen type I, bone \sialoprotein, receptor activator of NF-κB ligand and osteoprotegerin).	[57]
Merwinite[a]	Higher cellular viability and proliferation compare to HA, stimulate osteoblast differentiation				Dorsal ruffles and minor filopodia			No cytotoxicity	[160]

Abbreviations: Col1: Collagen type 1; OPN: Osteopontin; ALP: Alkaline phosphatase; β-TCP: β-tricalcium phosphate; BMP-2: Bone morphogenetic protein; RUNX2: Runt-related transcription factor 2; mRNA: Messenger ribonucleic acid; HA: Hydroxyapatite.

[a] Osteoblast like cells.

nanoindentation tests, whereas the hardness and modulus of the HA coating were 3.8 ± 3.1 GPa and 66.8 ± 39.3 GPa, respectively. The in vitro investigation demonstrated that the osteointegration of MG63 cells on baghdadite coating was significantly better than the HA coating and pure titanium surfaces, suggesting the beneficial biological features of the baghdadite coating foster the proliferation of MG63 cells.

Another study conducted by Bakhsheshirad et al. [54] examined the antibacterial activities and corrosion resistance of a coated magnesium (Mg) alloy made from zinc oxide combined with baghdadite by physical vapor deposition (PVD) and electrophoretic deposition (EPD). The ZnO-coated Mg alloy samples and the naked sample in simulated bodily fluid solution, the $ZnO/Ca_3ZrSi_2O_9$-coated specimen exhibited excellent corrosion resistance. It is apparent that after the coatings of ZnO and $ZnO/Ca_3ZrSi_2O_9$ were deposited on the Mg alloy substrate with 1603 mVSCE (corrosion potential), the corrosion potential shifted to a more noble direction, reaching −1436 mVSCE and −1073 mVSCE, respectively. In addition, ZnO and $ZnO/Ca_3ZrSi_2O_9$ coatings exhibited large

zones of inhibition against escherichia coli, klebsiella pneumonia, and shigella dysenteriae compared to the uncoated and coated samples. Also, the authors reported that the compressive strengths of the ZnO-coated and $ZnO/Ca_3ZrSi_2O_9$-coated samples were measured 148.2 and 170.6 MPa, respectively, only after 10 days of soaking in the SBF.

A study by Karimi et al. [103] examined the osteogenic potential of adipose-derived mesenchymal stem cells (AD-MSCs) derived from adipose tissue by coating baghdadite (1% w/v, solution of baghdadite) on an electrospun poly-L-lactic acid (PLLA) surface treated with plasma. That study showed that PLLA-baghdadite successfully activated high efficacy in osteogenesis-related genes (RUNX2). PLLA-baghdadite nanofibers possessed higher calcium content and more significant alkaline phosphatase activity than polystyrene tissue culture matrices. It has been shown that oxygen plasma treatment produces anionic groups on the surface of the scaffold. Ca^{2+} is electrostatically attracted to these anionic groups. Despite the growing trend of cell proliferation on PLLA-baghdadite scaffolds, the results of the MTT test reveal that the cell
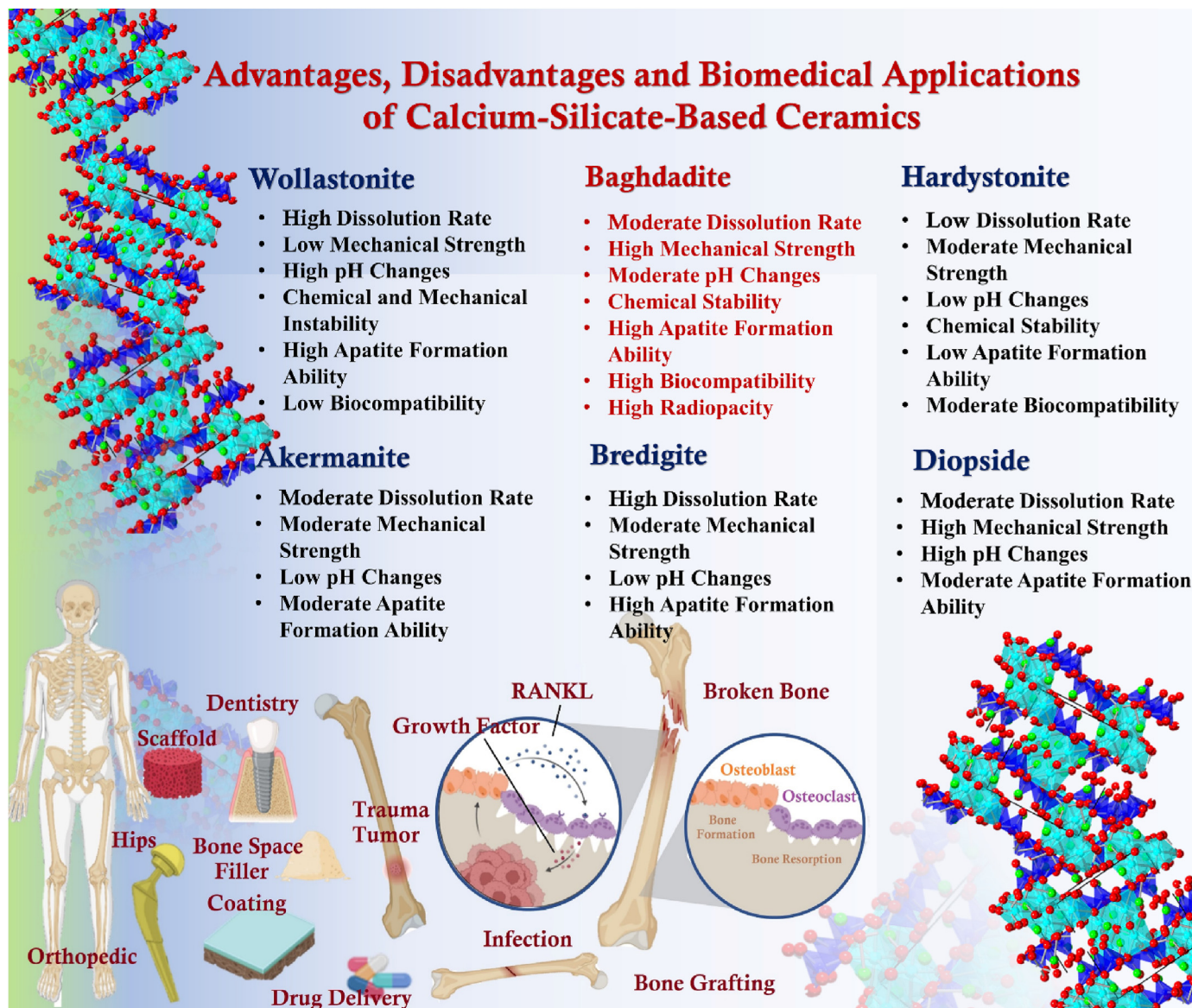
Fig. 8. Comparing advantages, disadvantages and biomedical applications of calcium-silicate-based ceramics.

proliferation rate is lower on PLLA-baghdadite. It was reported that during osteogenic differentiation from days 1–14, alkaline phosphatase was increased in cells grown on all scaffold groups and dropped afterwards. Therefore, baghdadite did not affect osteocalcin expression in that composite.

3.7. Simulation

Simulations provide a means of testing the validity of theories and models. Technically, the simulations produce results that are directly comparable with real-world experiments. Due to the many particles in molecular systems, analytically determining their characteristics is nearly impossible. This problem is solved using molecular dynamics simulation (MD). The Molecular Dynamics (MD) method is a powerful tool for describing how atomic structures behave mechanically. This method of computation can successfully describe several atomic phenomena. Bu et al. [119] have reported that this method can be used to explain the influence of water molecules on the mechanical behavior of the baghdadite matrix. For this purpose, several physical characteristics such as temperature, total energy, ultimate strength, Young's modulus, and interaction energy were recorded after 10 ns. Based on the molecular

dynamics results, it is evident that the H_2O molecules affect the atomic properties of the baghdadite matrix, decreasing the mechanical characteristics of the structure. Using numerical methods, the strength and Young's modulus of the baghdadite matrix with and without water molecules were reported at 110.56 MPa, 137.96 MPa, and 121.24 MPa/157.43 MPa, respectively. These results reveal the significance of the moisture environment on the mechanical behavior of baghdadite-based structures. They confirmed that this atomic matrix could be used as a bone treatment target for clinical purposes. As bone grows in the baghdadite scaffolds over time in the biological environment [78], researchers have suggested constructing a mechanical model that can be used to measure their stiffness and strength. In their paper, the authors used linear elasticity and beam theory to argue that the ingrowth of bone is the source of increased stiffness and strength. Model validation and experimental data revealed that their proposed relatively simple model accounted for the overall trends and thus could be used to attempt a rapid assessment of stiffness and strength amplification due to bone ingrowth. This model can be particularly beneficial for anticipating quality at different locations after surgery without mechanical tests. In prior research [120,121] primary temperatures (in the range of 250–350 K) and pressure (in the range of 0–10 bar) were not examined in detail for

baghdadite-based nanostructures. In a study, Liu et al. [122] investigated the influence of temperature and pressure variations on the mechanical conductivity of the baghdadite matrix with nanoscale dimensions using the MD method.

According to the author's claim, the MD was used for the first time to describe the baghdadite's mechanical/atomic behavior at various temperatures and pressures. It is possible to determine baghdadite's atomic-level time evolution through MD simulations. Those calculations recorded various physical values, including total energy, final strength, temperature, stress-strain curve, and Young's modulus. The simulation results showed that temperature and pressure increase the mechanical properties of baghdadite nanostructures. Based on the results, the strength and modulus of the defined structure were reported at 131.40 MPa, 159.43 MPa, and 115.15 MPa, 139.72 MPa as temperature and pressure increased. The increase in pressure and temperature at the beginning of the process will decrease the mechanical properties of nanostructures. In clinical applications, the initial condition must be considered when examining the mechanical behavior of baghdadite-based nanostructures [122].

4. Comparing baghdadite ceramic with other calcium silicate-based/commercial ceramics, and natural bone

Regeneration and repair through the incorporation of various elements, including zirconium (Zr), zinc (Zn), iron (Fe), strontium (Sr), copper (Cu), titanium (Ti), and magnesium (Mg) in the $CaSiO_3$-based ceramic. The most important calcium-silicate-based ceramics are wollastonite ($CaSiO_3$), diopside ($CaMgSi_2O_6$) [123,124], bredigite ($Ca_7MgSi_4O_{16}$) [125,126], merwinite ($Ca_3MgSi_2O_8$) [127,128], hardystonite ($Ca_2ZnSi_2O_7$) [129,130], baghdadite ($Ca_3ZrSi_2O_9$) [102,108], akermanite ($Ca_2MgSi_2O_7$) [131,132], their modification with doping elements (nonstoichiometric ceramics), and composites of these ceramics [4,133]. This section will compare the important properties of baghdadite ceramic with different calcium-silicate-based ceramics, including mechanical properties, degradation, pH controllability, in vitro and in vivo evaluation relating to bone regeneration and vascularization capability, and radiopacity. It is well-known that the composition of calcium-silicate-based ceramics is one of the key parameters affecting their properties and determining their biocompatibility, bioactivity, and biodegradability. Furthermore, it has been shown that the incorporation and presence of specific elements into the calcium-silicate ceramics structure affect not only their composition and structure stability but also their phase distribution and microstructure. By designing the molecular precursor, it is possible to alter and adjust the macroscopic and microscopic chemical, physical, and mechanical properties of calcium-silicate-based ceramics to a significant degree. Calcium-silicate-based ceramics groups such as Ca–Zr–Si, Ca–Mg–Si, and Ca–Zn–Si, synthesized from precursors including Ca, Si, and x (incorporating metallic elements into the structure of calcium-silicate-based ceramics), which has prevented oxide phase separating (like ZrO_2, MgO, CaO, ZnO, and SiO_2) during sintering due to the strong bonding between silicon, calcium, oxygen, and metal atoms. The simplified crystal structures of some calcium-silicate-based ceramics are illustrated in Fig. 6. As shown in this figure, the oxygen atoms can be considered as a coupler for both x and Ca ions to silicon elements. Depending on the type and number of (x) elements, the atomic bond vibration and d spacing lead to distinct classes of calcium-silicate-based ceramics.

Fig. 7 shows the effect of incorporating various ions on the mechanical properties of porous and dense calcium-silicate-based ceramics compared to baghdadite and commercial bioceramic substitutes [32]. As evident in Fig. 7, calcium-silicate-based ceramics, especially diopside and baghdadite, achieve significantly better mechanical properties, including higher bending strength and fracture toughness, than commercial bioceramic substitutes [31,38]. Diopside and baghdadite ceramic possessed the highest strength and Young's modulus of all calcium-silicate-based ceramics in dense and porous forms (Fig. 7). The other

calcium-silicate-based ceramics (dense and porous) showed bending and compression strengths in the range of 50–156 and 0.06–0.53 MPa and fracture toughness in the range of 0.5–1.57 MPa m$^{0.5}$, which are higher than commercial bioceramics and bioactive glasses. Variations in strength among different types of calcium-silicate-based ceramics could be attributed to some factors, including differences in the crystal structure and ionic interactions between the dopant ions and oxides in Ca–Si ceramic system. Furthermore, by changing the sintering properties of these types of ceramics, another influence of incorporating ions into the Ca–Si system may be the mechanical properties. As shown in Fig. 7 (A-C), the bending and compressive strengths of dense and porous hydroxyapatite, β-TCP, and bio-glass (45S5) are reported in the range of 100–160, 118–133, 83, 14.61, 3.4, and 0.42–0.6 MPa, respectively. The mechanical properties of baghdadite ceramic reached the lower end of the reported range for cortical and trabecular bone. However, this ceramic is not suitable for high-load-bearing musculoskeletal applications.

Calcium-silicate-based ceramics have also received considerable attention for their ability to efficiently induce bone-like apatite formation, stimulate osteogenesis, and generate bone tissue regeneration by releasing bioactive ionic products. Table 4 shows the results of apatite formation ability, degradability, and in vitro and in vivo properties for calcium-silicate-based ceramics compared to baghdadite. Almost all calcium-silicate-based ceramics have shown apatite formation ability. However, the rate of this function is related to the release of ions in the surrounding medium [12,13,25,38,134–141,149–151]. As shown in Table 4, some of those ceramics have shown the highest level of bioactivity. This behavior was entirely determined by the type of ions and their concentration in the ceramics. As can be observed, incorporating Mg and Zn ions into the calcium-silicate ceramic structure decreases the apatite formation ability compared to wollastonite due to a decrease in the concentration of Ca and Si ions. However, bredigite and other Mg-based calcium-silicate ceramics (akermanite, merwinite) exhibit a rapid dissolution rate and high apatite formation ability. No noticeable apatite formation ability could be observed for hardystonite ceramics, and its dissolution rate is also low, which is referred to its crystal structure [143]. Furthermore, the Zn ion has no vital role in apatite formation. The Zn ion is distinguished due to its antimicrobial effect, which promotes angiogenesis and homeostasis and is vital in the formation, development, and bone mineralization processes [144]. Baghdadite ceramic has shown good apatite formation ability with appropriate degradability.

Another strategy to modify the physicochemical and biomechanical properties of the $CaSiO_3$ is using doping strategy with dilute ions doped, which fabricate the nonstoichiometric ion doped-$CaSiO_3$ [148]. To further regulate the biodegradation and bioinductivity of the $CaSiO_3$ (CSi), the dilute doping of nonstoichiometric elements like Mg, Sr, Zn, or Mn was identified as feasible, which was readily conducted via the simple incorporation of doping elements into the $CaSiO_3$ precursor [145–148]. The doping of those ions led to different degradation, pH changes, and ion release behaviors of those materials. These CSi scaffolds demonstrated different degrees of efficiency in enhancing the osteogenic and angiogenic differentiation of BMSCs in vitro and promoting vascularization and new bone formation in vivo [145,146]. Table 4 shows the in vitro and in vivo properties of these ceramics. The differences between the ceramics in physicochemical and biological properties were ascribed to the different radii of doped ions and the bonding strength [146]. In general, the results across a range of experimental studies indicated reduced weight loss, ion release, and alkalinity for different types of dilute ions doped-CSi compared to $CaSiO_3$ when tested under similar conditions (Table 4). For instance, the weight loss of wollastonite scaffold has been reported to be up to 30 wt% by 7 days and raised the aqueous media pH to 9.3 [146]. Incorporating Mg, Mn, Zn, and Sr divalent ions into the structure of $CaSiO_3$ ceramic decreased the weight loss by around 40–50% compared to pure $CaSiO_3$ [144–147]. Compared to baghdadite, dilute ions doped-CSi scaffolds exhibited a higher dissolution rate (up to 20 wt% at day 7) and pH changes (8–9), while baghdadite exhibited lower weight loss (~9 wt% after 7 days) without raising the pH to toxic

levels (less than 8).

As can be seen in Fig. 6C, for the dilute ion doped-CSi scaffolds (Zn, Mg, Mn, and Sr–CSi) with porosity in the range of 40–50%, compressive strength was reported in the range of 0.02–120 MPa [146,148,152,153]. Compared to baghdadite ceramics with 80–90% porosity, which have shown compressive strength in a narrow range (0.6–2 MPa), wide range of compressive strength of different types of diluted ions doped-CSi scaffolds could be attributed to other factors, such as fabrication method, differences in the radius, and ionic interactions between the dopant ions. The mechanical strength of baghdadite scaffolds is affected mainly by the porosity of the scaffold. At the same time, it seems that the dilute ions doped-CSi scaffolds are more affected by the fabrication methods and types of dopant ions (in constant porosity) [146]. Based on the literature, the amount of porosity of dilute ions doped-CSi is another reason for their higher compressive strength compared to baghdadite [24]. However, stress shielding might happen due to a stiffness mismatch between the implant and bone for these types of scaffolds. The mechanical properties of these ceramics are still insufficient to match the mechanical properties of cancellous bone.

In general, comparing the results of stochiometric and non-stoichiometric ceramics would be difficult. Although dilute ions doped-CaSiO$_3$ ceramics showed appreciable mechanical and degradation rate properties, there is a lack of in-depth in vivo and in vitro and mechanical studies of these types of ceramics to compare with stoichiometric composition ceramics such as baghdadite, diopside, hardystonite, etc.

The in vitro interactions of different calcium-silicate-based ceramics have been evaluated using a range of cells and implant types (as shown in Table 4) [11,56,57,137,154–163]. Ca, Si, Sr, Mg, Zr and Zn are most of the ions released by bioactive calcium-silicate-based ceramics that play a crucial role in bone formation (e.g., Mg, Si, Ca, Zr) and angiogenesis (e.g., Sr, Zn), which both of these features are necessary for the successful reconstruction of vascularized bone tissue [158,161,164]. Calcium-silicate-based ceramics doped with Zn, Ti and Zr showed lower release rates than Mg, Sr and Cu from other calcium-silicate-based ceramics under similar experimental conditions. Comparing the ion release rates of metal ions in baghdadite and hardystonite ceramics has shown that release rates of Zr ions in baghdadite are independent of Ca and Si ions release, while hardystonite reveals the lowest release rates for all Ca, Zn, and Si elements among all calcium-silicate-based ceramics. Ion release can be considered the primary mechanism to enhance cell interactions and in vivo properties of ceramics, influencing the biocompatibility property. Based on the in vitro results, Ca, Zn, Si, and Zr ions all enhance osteogenic and angiogenic gene expression in a range of all human bone and blood cell types, which means these ceramics are cell-friendly and provide an appropriate environment for cell viability, proliferation, attachment, and differentiation. However, the high biocompatibility of baghdadite and the moderate one for hardystonite can be explained by the ion release rate, in which baghdadite can have more control on the concentration of Ca, Si, and Zr released, while the releasing rates of ions in hardystonite are dependent on each other, and it is too slow compared to baghdadite. This material cannot provide enough ions to enhance cell interactions with ceramic. Therefore, hardystonite is more biostable and less biocompatible compared to baghdadite [40,57]. The dissolution rate of calcium-silicate-based ceramics in an aqueous environment is generally a function of the dopant ion valency [77] and metal-oxide bonding strength [78], although the exact roles of dopant ions and oxides in modulating the in vitro degradation behavior of these types of ceramics requires further investigation.

In Table 4, it is shown that ion release leads to pH changes and creates an alkaline environment for several types of calcium-silicate-based ceramics in physiological. Based on the literature [11,136,154,160,165], wollastonite, diopside, merwinite, and baghdadite were reported to raise the pH from 7.4 to a range of 7.8–8.6 after 7 days of soaking in SBF. By demonstrating attachment, proliferation, gene expression, and enzyme activity, calcium-silicate-based ceramics can influence in vitro cell behavior but not exhibit a linear dose-response relationship [4,166]. As shown in Table 4, akermanite, diopside, mervinite, and bredigite promoted osteogenic gene expression in osteoblast cells. Compared to β-TCP or HA, and all calcium-silicate-based ceramics, baghdadite, enhanced osteoblast adhesion, proliferating cells and promoted osteogenic differentiation, alkaline phosphatase, osteopontin, bone sialoprotein, and osteocalcin [154,157,162,163].

The in vivo performance of several calcium-silicate ceramics (scaffold or powder) has been reported in Table 4. Generally speaking, all the studies [56,155–157,163] demonstrated better bone reformation results with calcium-silicate-based ceramic implants than with calcium phosphate implants [158,159]. Both small and large animal models tolerated the calcium-silicate-based ceramic implants without any evidence of inflammatory reactions or fibrous tissue forming at the surface of the implant [11,160]. Baghdadite scaffolds achieved complete bridging of large-sized defects by stimulating the rapid regeneration of new bone along the defect edges [56,159]. Additionally, this scaffold facilitated new bone growth into the pores, thus enhancing the scaffold's integration with the host bone tissue [63]. In contrast, the calcium phosphate control samples showed minimal bone penetration into the scaffolds' pores, while the bone's growth was restricted outside the scaffold [142,161].

According to the evidence available on the performance of baghdadite implant in various orthotopic animal models, it may provide better reconstructive results in orthopedic applications than current bone substitutes made from calcium phosphates or bioactive glasses. These advantages result from their mechanical properties, degradation characteristics, and capacity to increase cell interaction, as discussed in these sections [161,162].

An XMAC value is determined by its elemental composition, with heavier elements having higher XMAC values. As a result, a high XMAC indicates that the material is more radiopaque and, therefore, more visible by non-invasive means such as X-rays and computed tomography. In the energy range of 20 keV, the calculated XMAC for wollastonite, diopside, akermanite, bredigite, hardystonite, and baghdadite is 5.94, 4.27, 5.36, 6.62, 12.96, and 20.76, respectively [26]. Compared to the XMAC for bioglass 45S5 (4.09), hydroxyapatite (6.38), tricalcium phosphate (6.49), cortical bone (4), and among all calcium-silicate ceramics, baghdadite has shown the highest XMAC, which is the most vital property for implants [26]. This is often overlooked during biomaterial design and characterization. In a nutshell, the advantages and disadvantages of calcium-silicate-based ceramics compared to baghdadite ceramics are shown in Fig. 8.

5. Limitations of baghdadite ceramic

The potential of using baghdadite for bone regeneration has been confirmed by several studies, aforementioned in previous sections, which showed the ability of this ceramic to achieve direct bonding with native bone, resulting in favorable in vitro and in vivo regeneration outcomes. However, several significant limitations of baghdadite have prevented its development as a bone substitute for clinical use. Firstly, the mechanical strength of baghdadite as bulk and porous scaffold monoliths is deficient. Although the mechanical properties of baghdadite ceramic have reached the lower end of the reported range for cortical and trabecular bone, this ceramic is still unsuitable for high load-bearing musculoskeletal applications. Secondly, the workability of pure baghdadite, like other bioceramics, is insufficient, and surgeons cannot shape baghdadite during surgery [8,9,46,167].

Moreover, shaping baghdadite reduces its reliability as far as mechanical properties are concerned. Also, despite the perfect biological properties of baghdadite, this ceramic suffers from poor antibacterial properties, resulting in implant infections and post-operative complications [77–79]. Unlike some commercial bioceramics, which are approved by the food and drug administration (FDA) to use routinely in clinical application, there is no clinical report and FDA approval for baghdadite ceramic. Still, this ceramic is in the experimental stage. Furthermore, this ceramic is limited in usage due to its inherent brittleness. Its low

resistance to the initiation and propagation of cracks is another problem of this ceramic. Although using baghdadite as a surface modifier has been shown to improve osseointegration and reduce the rate of corrosion and the release of toxic ions, there is still no consensus on the ideal value and surface roughness of baghdadite [118].

6. Summary and future perspectives

In recent years, extensive studies have been performed on various bioceramics in medical applications, particularly those based on calcium and silicate. Among all those ceramics, baghdadite bioceramics have demonstrated high apatite formation ability, biocompatibility, osteoinductivity, conductivity, controllable degradability, biocompatibility, good cellular interaction, and various advantages for bone regeneration and repair in medical applications and tissue engineering [11,69]. This ceramic's superior physical, biological, and mechanical properties result from incorporating bioactive Zr ions into the calcium-silicate ceramic [167]. The incorporation of Zr ions results in a more stable structure. Higher mechanical properties of this ceramic in comparison to other calcium-silicate-based ceramics make it ideal for a wide range of biological applications [78]. This ceramic has positively affected cellular activities like proliferation, adhesion, and differentiation by releasing Zr, Ca, and Si ions. Furthermore, baghdadite has been confirmed to stimulate osteogenesis, particularly in vivo. Combining baghdadite with other materials (organic or inorganic) is one of the best approaches to addressing issues with the currently available materials in the medical field. Using baghdadite as a filler, coating, or base matrix has been beneficial for producing composite biomaterials with improved properties [18,109,168]. Major advances have been achieved in this field by developing baghdadite-based composites with a great balance between implant architecture and biological, mechanical, and physical functions to fulfill all requirements of bone. As an illustration, the high bioactivity and biocompatibility of baghdadite ceramic can be combined with the high mechanical properties and cellular interaction of other bioactive materials for various applications in the biomedical field [12,81]. Recently, additive manufacturing technology has emerged to produce complex scaffold structures applicable to bone tissue engineering with the promise of custom-made implants. However, this technology has been slow in producing baghdadite scaffolds, and there is a room for advancement [79]. We speculate on several pathways in which new research might be conducted using baghdadite ceramics. First, due to the in-situ printing technology in vivo, the baghdadite-based composite might be developed by printing directly on the organs inside the body, where the natural environment provides necessary cues for tissue regeneration. Second, inks based on baghdadite that will be set in aqueous media without toxic additives and sintering will be developed to print baghdadite at room temperature and in physiological conditions [169,170]. Bone is composed of organic and inorganic material, and the main cells and molecules are located in the mineralized organic matrix in close interaction with the inorganic phase. Therefore, this technique could potentially embed metabolically active bone cells in bio-inks to bio-print a baghdadite-based scaffold directly into damaged tissue. Combining 3D-printed baghdadite ceramic with soft biomaterials like hydrogel would build biomimetic bone tissue constructs that replicate the bone's biophysical properties. Also, structures with vascularized networks could be generated in vitro [171]. Even though 3D printing is a valuable tool in producing complex structures with specific shapes for tissue engineering, the printed objects are quite different from native tissues. In other words, the printed constructs are completely static and do not alter their morphology in response to various environmental conditions. A new technology known as four-dimensional printing (or 4D) has emerged to overcome these issues, using smart materials to improve printed structures over the standard two-dimensional printing method. 4D bioprinting can use stimuli-responsive materials, wherein 3D printed scaffolds are designed to transform over time due to various environmental stimuli. It could be a novel, powerful, visionary, and promising application of the baghdadite-based composite in future studies. However, more development and study are required before the clinical application of this technology [172–174]. Generally, according to the reviewed studies on pure or composite baghdadite ceramics, these biomaterials can be promising candidates with high potential for developing various biomedical applications, from scaffolds and cement to coatings and fillers as biomedical implants. Therefore, as a novel ceramic, baghdadite can offer enhanced clinical outcomes in existing therapies. In order to produce promising biomedical devices, one or a combination of these systems may be selected depending on the application and the conditions.

Declaration of competing interest

The authors declare that they have no known competing financial interests or personal relationships that could have appeared to influence the work reported in this paper.

Data availability

The data that has been used is confidential.

Acknowledgments

Appendix A. Supplementary data

Supplementary data to this article can be found online at https://doi.org/10.1016/j.mtbio.2022.100473.
Advances on bioactive baghdadite for bone tissue engineering …

References

[1] J. Van der Stok, E.M.M. Van Lieshout, Y. El-Massoudi, G.H. Van Kralingen, P. Patka, Bone substitutes in The Netherlands–a systematic literature review, Acta Biomater. 7 (2011) 739–750.

[2] H. Mohammadi, M. Hafezi, N. Nezafati, S. Heasarki, A. Nadernezhad, S.M.H. Ghazanfari, M. Sepantafar, Bioinorganics in bioactive calcium silicate ceramics for bone tissue repair: bioactivity and biological properties, J. Ceram. Sci. Technol. 5 (2014) 1–12.

[3] E. Hjørting-Hansen, Bone grafting to the jaws with special reference to reconstructive preprosthetic surgery, Mund-, Kiefer-Und Gesichtschirurgie. 6 (2002) 6–14.

[4] P. Srinath, P. Abdul Azeem, K. Venugopal Reddy, Review on calcium silicate-based bioceramics in bone tissue engineering, Int. J. Appl. Ceram. Technol. 17 (2020) 2450–2464.

[5] M.-C. Lin, C.-C. Chen, I.-T. Wu, S.-J. Ding, Enhanced antibacterial activity of calcium silicate-based hybrid cements for bone repair, Mater. Sci. Eng. C 110 (2020), 110727.

[6] G. Fernandez de Grado, L. Keller, Y. Idoux-Gillet, Q. Wagner, A.-M. Musset, N. Benkirane-Jessel, F. Bornert, D. Offner, Bone substitutes: a review of their

characteristics, clinical use, and perspectives for large bone defects management, J. Tissue Eng. 9 (2018), 2041731418776819.

[7] A. Arefpour, M. Kasiri-Asgarani, A. Monshi, S. Karbasi, A. Doostmohammadi, S. Rostami, In vitro bioactivity of baghdadite-coated PCL–graphene nanocomposite scaffolds: mechanism of baghdadite and apatite formation, Mater. Technol. 36 (2021) 761–770.

[8] S. Sadeghzade, F. Shamoradi, R. Emadi, F. Tavangarian, Fabrication and characterization of baghdadite nanostructured scaffolds by space holder method, J. Mech. Behav. Biomed. Mater. 68 (2017) 1–7.

[9] Y.J. No, I. Holzmeister, Z. Lu, S. Prajapati, J. Shi, U. Gbureck, H. Zreiqat, Effect of baghdadite substitution on the physicochemical properties of brushite cements, Materials 12 (2019) 1719.

[10] T.C. Schumacher, A. Aminian, E. Volkmann, H. Lührs, D. Zimnik, D. Pede, W. Wosniok, L. Treccani, K. Rezwan, Synthesis and mechanical evaluation of Sr-doped calcium-zirconium-silicate (baghdadite) and its impact on osteoblast cell proliferation and ALP activity, Biomed. Mater. 10 (2015), 55013.

[11] S.I. Roohani-Esfahani, C.R. Dunstan, B. Davies, S. Pearce, R. Williams, H. Zreiqat, Repairing a critical-sized bone defect with highly porous modified and unmodified baghdadite scaffolds, Acta Biomater. 8 (2012) 4162–4172.

[12] H.R. Bakhsheshi-Rad, E. Hamzah, A.F. Ismail, M. Aziz, Z. Hadisi, M. Kashefian, A. Najafinezhad, Novel nanostructured baghdadite-vancomycin scaffolds: in-vitro drug release, antibacterial activity and biocompatibility, Mater. Lett. 209 (2017) 369–372.

[13] S. Sadeghzade, R. Emadi, T. Ahmadi, F. Tavangarian, Synthesis, characterization and strengthening mechanism of modified and unmodified porous diopside/baghdadite scaffolds, Mater. Chem. Phys. 228 (2019) 89–97.

[14] F. Tavangarian, C.A. Zolko, S. Sadeghzade, M. Fayed, K. Davami, Fabrication, mechanical properties and in-vitro behavior of Akermanite bioceramic, Materials 13 (2020), https://doi.org/10.3390/ma13214887.

[15] S. Punj, J. Singh, K. Singh, Ceramic biomaterials: properties, state of the art and future prospectives, Ceram. Int. 47 (2021) 28059–28074.

[16] P. Ducheyne, Comprehensive Biomaterials, Elsevier, 2015.

[17] C. Castells-Sala, M. Alemany-Ribes, T. Fernández-Muiños, L. Recha-Sancho, P. López-Chicón, C. Aloy-Reverté, J. Caballero-Camino, A. Márquez-Gil, C.E. Semino, Current applications of tissue engineering in biomedicine, J. Biochips Tissue Chips (2013) 1.

[18] D.Q. Pham, C.C. Berndt, J. Cizek, U. Gbureck, H. Zreiqat, Z. Lu, A.S.M. Ang, Baghdadite coating formed by hybrid water-stabilized plasma spray for bioceramic applications: mechanical and biological evaluations, Mater. Sci. Eng. C 122 (2021), 111873.

[19] Y.-C. Chiu, M.-Y. Shie, Y.-H. Lin, A.K.-X. Lee, Y.-W. Chen, Effect of strontium substitution on the physicochemical properties and bone regeneration potential of 3D printed calcium silicate scaffolds, Int. J. Mol. Sci. 20 (2019) 2729.

[20] C.-Y. Chen, M.-Y. Shie, A.K.-X. Lee, Y.-T. Chou, C. Chiang, C.-P. Lin, 3D-printed ginsenoside Rb1-Loaded mesoporous calcium silicate/calcium sulfate scaffolds for inflammation inhibition and bone regeneration, Biomedicines 9 (2021) 907.

[21] S. Sadeghzade, R. Emadi, H. Ghomi, Mechanical alloying synthesis of forsterite-diopside nanocomposite powder for using in tissue engineering, Ceramics 59 (2015) 1–5.

[22] S. Sadeghzade, R. Emadi, F. Tavangarian, M. Naderi, Fabrication and evaluation of silica-based ceramic scaffolds for hard tissue engineering applications, Mater. Sci. Eng. C 71 (2017) 431–438.

[23] S. Sadeghzade, R. Emadi, F. Tavangarian, Evaluation of mechanical properties, biodegradability and bioactivity of forsteritediopside scaffolds coated by polycaprolacton fumarate, in: Mater. Sci. Technol. 2019, MS T 2019, Materials Science and Technology, 2019, pp. 1310–1317.

[24] S. Sadeghzade, R. Emadi, Improving the mechanical and bioactivity of hydroxyapatite porous scaffold ceramic with diopside/forstrite ceramic coating, Nanomedicine J 6 (2019) 50–54.

[25] S. Zhao, L. Wang, W. Jiang, J. Zhang, L. Chen, Mechanical properties of CaSiO3/Ti3SiC2 composites and hydroxyapatite forming ability in simulated body fluid, Mater. Trans. 49 (2008) 2310–2314.

[26] Y.J. No, J.J. Li, H. Zreiqat, Doped calcium silicate ceramics: a new class of candidates for synthetic bone substitutes, Materials 10 (2017) 153.

[27] S. Sadeghzade, R. Emadi, F. Tavangarian, A. Doostmohammadi, In vitro evaluation of diopside/baghdadite bioceramic scaffolds modified by polycaprolactone fumarate polymer coating, Mater. Sci. Eng. C 106 (2020), 110176.

[28] Z. Zhang, W. Li, Y. Liu, Z. Yang, L. Ma, H. Zhuang, E. Wang, C. Wu, Z. Huan, F. Guo, Design of a biofluid-absorbing bioactive sandwich-structured Zn–Si bioceramic composite wound dressing for hair follicle regeneration and skin burn wound healing, Bioact. Mater. 6 (2021) 1910–1920.

[29] B. Aghajani, E. Karamian, B. Hosseini, Hydroxyapatite-Hardystonite nanocomposite scaffolds prepared by the replacing the polyurethane polymeric sponge technique for tissue engineering applications, Nanomedicine J 4 (2017) 254–261.

[30] S. Mehrafzoon, S.A. Hassanzadeh-Tabrizi, A. Bigham, Synthesis of nanoporous Baghdadite by a modified sol-gel method and its structural and controlled release properties, Ceram. Int. 44 (2018) 13951–13958.

[31] H. Jodati, B. Yilmaz, Z. Evis, Calcium zirconium silicate (baghdadite) ceramic as a biomaterial, Ceram. Int. 46 (2020) 21902–21909.

[32] S. Sadeghzade, R. Emadi, S. Labbaf, Hardystonite-diopside nanocomposite scaffolds for bone tissue engineering applications, Mater. Chem. Phys. 202 (2017) 95–103.

[33] S. Sadeghzade, R. Emadi, S. Labbaf, Fabrication and evaluation of the mechanical and bioactivity properties of a nano structure-hardystonite scaffold by the space holder method, J. Adv. Mater. Eng. 37 (2018) 55–67.

[34] H.M. Al-Hermezi, D. McKie, A.J. Hall, Baghdadite, a new calcium zirconium silicate mineral from Iraq, Mineral. Mag. 50 (1986) 119–123.

[35] C. Biagioni, E. Bonaccorsi, N. Perchiazzi, S. Merlino, Single Crystal Refinement of the Structure of Baghdadite from Fuka (Okayama Prefecture, Japan), 2010.

[36] M. Ficheux, E. Burov, G. Aquilanti, N. Trcera, V. Montouillout, L. Cormier, Structural evolution of high zirconia aluminosilicate glasses, J. Non-Cryst. Solids 539 (2020), 120050.

[37] J.R. Plaister, J. Jansen, R.A.G. De Graaff, D.J.W. Ijdo, Structure determination of Ca3HfSi2O9 and Ca3ZrSi2O9 from powder diffraction, J. Solid State Chem. 115 (1995) 464–468.

[38] T.C. Schumacher, E. Volkmann, R. Yilmaz, A. Wolf, L. Treccani, K. Rezwan, Mechanical evaluation of calcium-zirconium-silicate (baghdadite) obtained by a direct solid-state synthesis route, J. Mech. Behav. Biomed. Mater. 34 (2014) 294–301.

[39] S. Sadeghpour, A. Amirjani, M. Hafezi, A. Zamanian, Fabrication of a novel nanostructured calcium zirconium silicate scaffolds prepared by a freeze-casting method for bone tissue engineering, Ceram. Int. 40 (2014) 16107–16114.

[40] Y. Ramaswamy, C. Wu, H. Zhou, H. Zreiqat, Biological response of human bone cells to zinc-modified Ca-Si-based ceramics, Acta Biomater. (2008), https://doi.org/10.1016/j.actbio.2008.04.014.

[41] Y. Chen, S.-I. Roohani-Esfahani, Z. Lu, H. Zreiqat, C.R. Dunstan, Zirconium ions up-regulate the BMP/SMAD signaling pathway and promote the proliferation and differentiation of human osteoblasts, PLoS One 10 (2015), e0113426.

[42] N.J. Hallab, S. Anderson, M. Caicedo, J.J. Jacobs, Zirconium and Niobium Affect Human Osteoblasts, Fibroblasts, and Lymphocytes in a Similar Manner to More Traditional Implant Alloy Metals, ASTM International, 2006.

[43] A. Moghanian, M. Zohourfazeli, M.H.M. Tajer, The effect of zirconium content on in vitro bioactivity, biological behavior and antibacterial activity of sol-gel derived 58S bioactive glass, J. Non-Cryst. Solids 546 (2020), 120262.

[44] Y. Zhu, Y. Zhang, C. Wu, Y. Fang, J. Yang, S. Wang, The effect of zirconium incorporation on the physiochemical and biological properties of mesoporous bioactive glasses scaffolds, Microporous Mesoporous Mater. 143 (2011) 311–319.

[45] F.A. Soureshjani, M.R. Nilforoushan, H. Sharifi, A. Arefpour, A. Doostmohammadi, Improvement in mechanical and biological performance of porous baghdadite scaffold by applying chitosan coating, Appl. Phys. A 127 (2021) 1–12.

[46] A. Arefpour, M. Zolfaghari Baghbaderani, A. Shafieirad, M. Kasiri-Asgarani, A. Monshi, S. Karbasi, A. Doostmohammadi, A. Shahsavar Goldanlou, Mechanical behaviour, hybridisation and osteoblast activities of novel baghdadite/PCL-graphene nanocomposite scaffold: viability, cytotoxicity and calcium activity, Mater. Technol. (2021) 1–15.

[47] Y.J. No, T. Nguyen, Z. Lu, M. Mirkhalaf, F. Fei, M. Foley, H. Zreiqat, Development of a bioactive and radiopaque bismuth doped baghdadite ceramic for bone tissue engineering, Bone 153 (2021), 116147.

[48] A. Sidike, I. Kusachi, N. Yamashita, Yellow fluorescence from baghdadite and synthetic Ca 3 (Zr, Ti) Si 2 O 9, Phys. Chem. Miner. 32 (2006) 665–669.

[49] K. Dul, A. Koleżyński, M. Sitarz, D. Madej, Vibrational spectra of a baghdadite synthetic analogue, Vib. Spectrosc. 76 (2015) 1–5.

[50] A. Arefpour, M. Kasiri-Asgarani, A. Monshi, A. Doostmohammadi, S. Karbasi, Fabrication, characterization and examination of in vitro of baghdadite nanoparticles for biomedical applications, Mater. Res. Express 6 (2019), 95411.

[51] H.R. Bakhsheshi-Rad, E. Hamzah, A.F. Ismail, M. Aziz, M. Kasiri-Asgarani, E. Akbari, S. Jabbarzare, A. Najafinezhad, Z. Hadisi, Synthesis of a novel nanostructured zinc oxide/baghdadite coating on Mg alloy for biomedical application: in-vitro degradation behavior and antibacterial activities, Ceram. Int. 43 (2017) 14842–14850.

[52] E. Karamian, A. Nasehi, S. Saber-Samandari, A. Khandan, Fabrication of hydroxyapatite-baghdadite nanocomposite scaffolds coated by PCL/Bioglass with polyurethane polymeric sponge technique, Nanomedicine J 4 (2017) 177–183.

[53] A. Khandan, A Novel Silicate Ceramic-Magnetite Nanocomposite for Biomedical Application, 2017.

[54] A. Arefpour, M. Kasiri-Asgarani, A. Monshi, S. Karbasi, A. Doostmohammadi, Baghdadite/Polycaprolactone nanocomposite scaffolds: preparation, characterisation, and in vitro biological responses of human osteoblast-like cells (Saos-2 cell line), Mater. Technol. 35 (2020) 421–432.

[55] Y. Liang, Y. Xie, H. Ji, L. Huang, X. Zheng, Excellent stability of plasma-sprayed bioactive Ca3ZrSi2O9 ceramic coating on Ti–6Al–4V, Appl. Surf. Sci. 256 (2010) 4677–4681.

[56] T. Luo, C. Wu, Y. Zhang, The in vivo osteogenesis of Mg or Zr-modified silicate-based bioceramic spheres, J. Biomed. Mater. Res., Part A 100 (2012) 2269–2277.

[57] Y. Ramaswamy, C. Wu, A. Van Hummel, V. Combes, G. Grau, H. Zreiqat, The responses of osteoblasts, osteoclasts and endothelial cells to zirconium modified calcium-silicate-based ceramic, Biomaterials 29 (2008) 4392–4402.

[58] J. He, J. Fang, P. Wei, Y. Li, H. Guo, Q. Mei, F. Ren, Cancellous bone-like porous Fe@ Zn scaffolds with core-shell-structured skeletons for biodegradable bone implants, Acta Biomater. 121 (2021) 665–681.

[59] M. Zhu, J. Fang, Y. Li, C. Zhong, S. Feng, X. Ge, H. Ye, X. Wang, W. Zhu, X. Lu, The synergy of topographical micropatterning and Ta| TaCu bilayered thin film on titanium implants enables dual-functions of enhanced osteogenesis and anti-infection, Adv. Healthc. Mater. 10 (2021), 2002020.

[60] R. Duan, S. Li, B. Cai, W. Zhu, F. Ren, M.M. Attallah, A high strength and low modulus metastable β Ti-12Mo-6Zr-2Fe alloy fabricated by laser powder bed fusion in-situ alloying, Addit. Manuf. 37 (2021), 101708.

[61] W.C. Billotte, Ceramic biomaterials, in: Biomaterials, CRC Press, 2007, pp. 1–2.

[62] H. Mohammadi, M. Sepantafar, N. Muhamad, A. Bakar Sulong, How does scaffold porosity conduct bone tissue regeneration? Adv. Eng. Mater. 23 (2021), 2100463.

[63] L.-C. Gerhardt, A.R. Boccaccini, Bioactive glass and glass-ceramic scaffolds for bone tissue engineering, Materials 3 (2010) 3867–3910.

[64] A.M. Cakmak, S. Unal, A. Sahin, F.N. Oktar, M. Sengor, N. Ekren, O. Gunduz, D.M. Kalaskar, 3D printed polycaprolactone/gelatin/bacterial cellulose/ hydroxyapatite composite scaffold for bone tissue engineering, Polymers 12 (2020) 1962.

[65] X. Wang, Z. Zhu, H. Xiao, C. Luo, X. Luo, F. Lv, J. Liao, W. Huang, Three-dimensional, MultiScale, and interconnected trabecular bone mimic porous tantalum scaffold for bone tissue engineering, ACS Omega 5 (2020) 22520–22528.

[66] S. Gautam, C. Sharma, S.D. Purohit, H. Singh, A.K. Dinda, P.D. Potdar, C.-F. Chou, N.C. Mishra, Gelatin-polycaprolactone-nanohydroxyapatite electrospun nanocomposite scaffold for bone tissue engineering, Mater. Sci. Eng. C 119 (2021), 111588.

[67] D. Zhao, F. Witte, F. Lu, J. Wang, J. Li, L. Qin, Current status on clinical applications of magnesium-based orthopaedic implants: a review from clinical translational perspective, Biomaterials 112 (2017) 287–302.

[68] X. Wang, M. Jiang, Z. Zhou, J. Gou, D. Hui, 3D printing of polymer matrix composites: a review and prospective, Compos. B Eng. 110 (2017) 442–458.

[69] M. Karimi, A. Asefnejad, D. Aflaki, A. Surendar, H. Baharifar, S. Saber-Samandari, A. Khanban, A. Khan, D. Toghraie, Fabrication of shapeless scaffolds reinforced with baghdadite-magnetite nanoparticles using a 3D printer and freeze-drying technique, J. Mater. Res. Technol. 14 (2021) 3070–3079.

[70] A. Khademhosseini, R. Langer, A decade of progress in tissue engineering, Nat. Protoc. 11 (2016) 1775–1781.

[71] A.R. Studart, U.T. Gonzenbach, E. Tervoort, L.J. Gauckler, Processing routes to macroporous ceramics: a review, J. Am. Ceram. Soc. 89 (2006) 1771–1789.

[72] J.-Y. Lee, J. An, C.K. Chua, Fundamentals and applications of 3D printing for novel materials, Appl. Mater. Today 7 (2017) 120–133.

[73] K. Lin, R. Sheikh, S. Romanazzo, I. Roohani, 3D printing of bioceramic scaffolds—barriers to the clinical translation: from promise to reality, and future perspectives, Materials 12 (2019) 2660.

[74] G.X. Gu, I. Su, S. Sharma, J.L. Voros, Z. Qin, M.J. Buehler, Three-dimensional-printing of bio-inspired composites, J. Biomech. Eng. 138 (2016).

[75] L.J. Kumar, P.M. Pandey, D.I. Wimpenny, 3D Printing and Additive Manufacturing Technologies, Springer, 2019.

[76] M.J. Zafar, D. Zhu, Z. Zhang, 3D printing of bioceramics for bone tissue engineering, Materials 12 (2019) 3361.

[77] Z. Lu, W. Zhang, Y.J. No, Y. Lu, S.M. Mirkhalaf Valashani, P. Rollet, L. Jiang, Y. Ramaswamy, C.R. Dunstan, X. Jiang, Baghdadite ceramics prevent senescence in human osteoblasts and promote bone regeneration in aged rats, ACS Biomater. Sci. Eng. 6 (2020) 6874–6885.

[78] M. Mirkhalaf, A. Dao, A. Schindeler, D.G. Little, C.R. Dunstan, H. Zreiqat, Personalized Baghdadite scaffolds: stereolithography, mechanics and in vivo testing, Acta Biomater. 132 (2021) 217–226.

[79] M. Mirkhalaf, X. Wang, A. Entezari, C.R. Dunstan, X. Jiang, H. Zreiqat, Redefining architectural effects in 3D printed scaffolds through rational design for optimal bone tissue regeneration, Appl. Mater. Today 25 (2021), 101168.

[80] P.N. De Aza, J.M. Fernandez-Pradas, P. Serra, In vitro bioactivity of laser ablation pseudowollastonite coating, Biomaterials 25 (2004) 1983. –1990.

[81] Z. Lu, G. Wang, I. Roohani-Esfahani, C.R. Dunstan, H. Zreiqat, Baghdadite ceramics modulate the cross talk between human adipose stem cells and osteoblasts for bone regeneration, Tissue Eng. 20 (2014) 992–1002.

[82] X. Zhang, P. Han, A. Jaiprakash, C. Wu, Y. Xiao, A stimulatory effect of Ca 3 ZrSi 2 O 9 bioceramics on cementogenic/osteogenic differentiation of periodontal ligament cells, J. Mater. Chem. B. 2 (2014) 1415–1423.

[83] P.L. Graney, S.-I. Roohani-Esfahani, H. Zreiqat, K.L. Spiller, In Vitro Modulation of Macrophage Behavior by Ceramic-Based Scaffolds, Annu. Meet. Soc. Biomater., 2015.

[84] J.J. Li, A. Akey, C.R. Dunstan, M. Vielreicher, O. Friedrich, D.C. Bell, H. Zreiqat, Effects of material–tissue interactions on bone regeneration outcomes using baghdadite implants in a large animal model, Adv. Healthc. Mater. 7 (2018), 1800218.

[85] P.L. Graney, S.-I. Roohani-Esfahani, H. Zreiqat, K.L. Spiller, In vitro response of macrophages to ceramic scaffolds used for bone regeneration, J. R. Soc. Interface 13 (2016), 20160346.

[86] S.L. Teitelbaum, Bone resorption by osteoclasts, Science 289 (2000) 1504–1508.

[87] A. Doostmohammadi, Z. Karimzadeh Esfahani, A. Ardeshirylajimi, Z. Rahmati Dehkordi, Zirconium modified calcium-silicate-based nanoceramics: an in vivo evaluation in a rabbit tibial defect model, Int. J. Appl. Ceram. Technol. 16 (2019) 431–437.

[88] N.R. Patel, P.P. Gohil, A review on biomaterials: scope, applications & human anatomy significance, Int. J. Emerg. Technol. Adv. Eng. 2 (2012) 91–101.

[89] T.W. Clyne, D. Hull, An Introduction to Composite Materials, Cambridge University Press, 2019.

[90] S.W. Tsai, H.T. Hahn, Introduction to Composite Materials, Routledge, 2018.

[91] M. Balasubramanian, Composite Materials and Processing, CRC Press, Boca Raton, 2014.

[92] M.-S. Scholz, J.P. Blanchfield, L.D. Bloom, B.H. Coburn, M. Elkington, J.D. Fuller, M.E. Gilbert, S.A. Muflahi, M.F. Pernice, S.I. Rae, The use of composite materials in modern orthopaedic medicine and prosthetic devices: a review, Compos. Sci. Technol. 71 (2011) 1791–1803.

[93] N. Ramesh, S.C. Moratti, G.J. Dias, Hydroxyapatite–polymer biocomposites for bone regeneration: a review of current trends, J. Biomed. Mater. Res. Part B Appl. Biomater. 106 (2018) 2046–2057.

[94] M.P. Prabhakaran, J.R. Venugopal, T. Ter Chyan, L.B. Hai, C.K. Chan, A.Y. Lim, S. Ramakrishna, Electrospun biocomposite nanofibrous scaffolds for neural tissue engineering, Tissue Eng. 14 (2008) 1787–1797.

[95] M. Swetha, K. Sahithi, A. Moorthi, N. Srinivasan, K. Ramasamy, N. Selvamurugan, Biocomposites containing natural polymers and hydroxyapatite for bone tissue engineering, Int. J. Biol. Macromol. 47 (2010) 1–4.

[96] D. Rana, M. Ramalingam, Ceramic nanofiber composites, in: Nanofiber Compos. Biomed. Appl., Elsevier, 2017, pp. 33–54.

[97] A. Khandan, E. Karamian, M. Mehdikhani-Nahrkhalaji, H. Mirmohammadi, A. Farzadi, N. Ozada, B. Heidarshenas, K. Zamani, Influence of spark plasma sintering and baghdadite powder on mechanical properties of hydroxyapatite, Procedia Mater. Sci. 11 (2015) 183–189.

[98] Y.J. No, S. Roohani-Esfahani, Z. Lu, T. Schaer, H. Zreiqat, Injectable radiopaque and bioactive polycaprolactone-ceramic composites for orthopedic augmentation, J. Biomed. Mater. Res. Part B Appl. Biomater. 103 (2015) 1465–1477.

[99] R.R. Sehgal, S.I. Roohani-Esfahani, H. Zreiqat, R. Banerjee, Nanostructured gellan and xanthan hydrogel depot integrated within a baghdadite scaffold augments bone regeneration, J. Tissue Eng. Regen. Med. 11 (2017) 1195–1211.

[100] F. Soleymani, R. Emadi, S. Sadeghzade, F. Tavangarian, Bioactivity behavior evaluation of PCL-chitosan-nanobaghdadite coating on AZ91 magnesium alloy in simulated body fluid, Coatings 10 (2020) 231.

[101] F. Soleymani, R. Emadi, S. Sadeghzade, F. Tavangarian, Applying baghdadite/ PCL/chitosan nanocomposite coating on AZ91 magnesium alloy to improve corrosion behavior, bioactivity, and Biodegradability, Coatings 9 (2019) 789.

[102] F. Pahlevanzadeh, H.R. Bakhsheshi-Rad, A.F. Ismail, M. Aziz, Apatite-forming ability, cytocompatibility, and mechanical properties enhancement of poly methyl methacrylate-based bone cements by incorporating of baghdadite nanoparticles, Int. J. Appl. Ceram. Technol. 16 (2019) 2006–2019.

[103] Z. Karimi, E. Seyedjafari, F.S. Mahdavi, S.M. Hashemi, A. Khojasteh, B. Kazemi, S. Mohammadi-Yeganeh, Baghdadite nanoparticle-coated poly l-lactic acid (PLLA) ceramics scaffold improved osteogenic differentiation of adipose tissue-derived mesenchymal stem cells, J. Biomed. Mater. Res., Part A 107 (2019) 1284–1293.

[104] D.A. Samani, A. Doostmohammadi, M.R. Nilforoushan, H. Nazari, Electrospun polycaprolactone/graphene/baghdadite composite nanofibres with improved mechanical and biological properties, Fibers Polym. 20 (2019) 982–990.

[105] Z. Jia, P. Xiu, S.-I. Roohani-Esfahani, H. Zreiqat, P. Xiong, W. Zhou, J. Yan, Y. Cheng, Y. Zheng, Triple-bioinspired burying/crosslinking interfacial coassembly strategy for layer-by-layer construction of robust functional bioceramic self-coatings for osteointegration applications, ACS Appl. Mater. Interfaces 11 (2019) 4447–4469.

[106] V. Abbasian, R. Emadi, M. Kharaziha, Biomimetic nylon 6-baghdadite nanocomposite scaffold for bone tissue engineering, Mater. Sci. Eng. C 109 (2020), 110549.

[107] F. Abbasi Soureshjani, M.R. Nilforoushan, H. Sharifi, A. Arefpour, A. Doostmohammadi, Improvement in mechanical and biological performance of porous baghdadite scaffold by applying chitosan coating, Appl. Phys. A 127 (2021) 1–12.

[108] S. Yadav, A. Ali, S. Krishnamurthy, P. Singh, R. Pyare, In-vitro analysis of bioactivity, hemolysis, and mechanical properties of Zn substituted Calcium Zirconium silicate (baghdadite), Ceram. Int. 47 (2021) 16037–16053.

[109] S. Vaez, R. Emadi, S. Sadeghzade, H. Salimijazi, M. Kharaziha, Electrophoretic deposition of chitosan reinforced baghdadite ceramic nano-particles on the stainless steel 316L substrate to improve biological and physical characteristics, Mater. Chem. Phys. 282 (2022), 125991.

[110] J.J. Li, S.-I. Roohani-Esfahani, C.R. Dunstan, T. Quach, R. Steck, S. Saifzadeh, P. Pivonka, H. Zreiqat, Efficacy of novel synthetic bone substitutes in the reconstruction of large segmental bone defects in sheep tibiae, Biomed. Mater. 11 (2016), 15016.

[111] Y.J. No, S. Roohaniesfahani, Z. Lu, J. Shi, H. Zreiqat, Strontium-doped calcium silicate bioceramic with enhanced in vitro osteogenic properties, Biomed, Materials 12 (2017), 35003.

[112] J. Wang, L. Zhang, X. Sun, X. Chen, K. Xie, M. Lin, G. Yang, S. Xu, W. Xia, Z. Gou, Preparation and in vitro evaluation of strontium-doped calcium silicate/gypsum bioactive bone cement, Biomed. Mater. 9 (2014), 45002.

[113] K. Lin, L. Xia, H. Li, X. Jiang, H. Pan, Y. Xu, W.W. Lu, Z. Zhang, J. Chang, Enhanced osteoporotic bone regeneration by strontium-substituted calcium silicate bioactive ceramics, Biomaterials 34 (2013) 10028–10042.

[114] M. Ajeesh, B.F. Francis, J. Annie, P.R.H. Varma, Nano iron oxide–hydroxyapatite composite ceramics with enhanced radiopacity, J. Mater. Sci. Mater. Med. 21 (2010) 1427–1434.

[115] T. Wu, S. Yang, T. Lu, F. He, J. Zhang, H. Shi, Z. Lin, J. Ye, Strontium ranelate simultaneously improves the radiopacity and osteogenesis of calcium phosphate cement, Biomed. Mater. 14 (2019), 35005.

[116] K.A. Khor, C.S. Yip, P. Cheang, Ti-6Al-4V/hydroxyapatite composite coatings prepared by thermal spray techniques, J. Therm. Spray Technol. 6 (1997) 109–115.

[117] X. Wang, Y. Zhou, L. Xia, C. Zhao, L. Chen, D. Yi, J. Chang, L. Huang, X. Zheng, H. Zhu, Fabrication of nano-structured calcium silicate coatings with enhanced stability, bioactivity and osteogenic and angiogenic activity, Colloids Surf. B Biointerfaces 126 (2015) 358–366.

[118] D.Q. Pham, C.C. Berndt, U. Gbureck, H. Zreiqat, V.K. Truong, A.S.M. Ang, Mechanical and chemical properties of Baghdadite coatings manufactured by atmospheric plasma spraying, Surf. Coating. Technol. 378 (2019), 124945.

[119] W. Bu, R. Sabetvand, M. Hekmatifar, S.M. Alizadeh, A. Arefpour, D. Toghraie, C.-H. Su, H.C. Nguyen, A. Khan, The computational study of moisture effect on mechanical behavior of baghdadite matrix via molecular dynamics approach, J. Mater. Res. Technol. 15 (2021) 2828–2836.

[120] A.M. Morega, A.A. Dobre, M. Morega, Numerical simulation of magnetic drug targeting with flow–structural interaction in an arterial branching region of interest, Comsol Conf (2010) 17–19.

[121] F. Bazin, E. Vachette, Case Study: Relevance of ASTM and ISTA Standard Shipping Simulation Studies for the Validation of Real World Shipping of Drug Substances, 2017.

[122] Q. Liu, O. Bykanova, R. Akhmadeev, S. Baghaie, M. Hekmatifar, A. Arefpour, R. Sabetvand, V. Borisov, The numerical study of pressure and temperature effects on mechanical properties of baghdadite-based nanostructure: molecular dynamics simulation, Sci. Rep. 12 (2022) 1–12.

[123] A. Kazemi, M. Abdellahi, A. Khajeh-Sharafabadi, A. Khandan, N. Ozada, Study of in vitro bioactivity and mechanical properties of diopside nano-bioceramic synthesized by a facile method using eggshell as raw material, Mater. Sci. Eng. C 71 (2017) 604–610.

[124] R. Choudhary, S.K. Venkatraman, A. Chatterjee, J. Vecstaudza, M.J. Yáñez-Gascón, H. Perez-Sanchez, J. Locs, J. Abraham, S. Swamiappan, Biomineralization, antibacterial activity and mechanical properties of biowaste derived diopside nanopowders, Adv. Powder Technol. 30 (2019) 1950–1964.

[125] M. Rahmati, M. Fathi, M. Ahmadian, Preparation and structural characterization of bioactive bredigite (Ca7MgSi4O16) nanopowder, J. Alloys Compd. 732 (2018) 9–15.

[126] A. Khandan, N. Ozada, S. Saber-Samandari, M.G. Nejad, On the mechanical and biological properties of bredigite-magnetite (Ca7MgSi4O16-Fe3O4) nanocomposite scaffolds, Ceram. Int. 44 (2018) 3141–3148.

[127] M.S. Collin, S. Sasikumar, Effect of fuel on biomineralization of merwinite, Mater. Lett. 304 (2021) 130660.

[128] H. Ghomi, Fabrication of highly porous merwinite scaffold using the space holder method, Int. J. Mater. Res. 111 (2020) 711–718.

[129] S. Sadeghzade, R. Emadi, F. Tavangarian, A. Doostmohammadi, The influence of polycaporolacton fumarate coating on mechanical properties and in vitro behavior of porous diopside-hardystonite nano-composite scaffold, J. Mech. Behav. Biomed. Mater. 101 (2020), 103445.

[130] S.S.R. Caballero, H. Elsayed, S. Tadier, A. Montembault, E. Maire, L. David, T. Delair, P. Colombo, L. Gremillard, Fabrication and characterization of hardystonite-chitosan biocomposite scaffolds, Ceram. Int. 45 (2019) 8804–8814.

[131] F. Wang, X. Wang, K. Ma, C. Zhang, J. Chang, X. Fu, Akermanite bioceramic enhances wound healing with accelerated reepithelialization by promoting proliferation, migration, and stemness of epidermal cells, Wound Repair Regen. 28 (2020) 16–25.

[132] A.K. Sharafabadi, M. Abdellahi, A. Kazemi, A. Khandan, N. Ozada, A novel and economical route for synthesizing akermanite (Ca2MgSi2O7) nano-bioceramic, Mater. Sci. Eng. C 71 (2017) 1072–1078.

[133] C. Wu, J. Chang, A review of bioactive silicate ceramics, Biomed. Mater. 8 (2013), 32001.

[134] C. Wu, J. Chang, W. Zhai, S. Ni, J. Wang, Porous akermanite scaffolds for bone tissue engineering: preparation, characterization, and in vitro studies, J. Biomed. Mater. Res. Part B Appl. Biomater. An Off. J. Soc. Biomater. Japanese Soc. Biomater. Aust. Soc. Biomater. Korean Soc. Biomater. 78 (2006) 47–55.

[135] T. Nonami, S. Tsutsumi, Study of diopside ceramics for biomaterials, J. Mater. Sci. Mater. Med. 10 (1999) 475–479.

[136] C. Wu, Y. Ramaswamy, H. Zreiqat, Porous diopside (CaMgSi2O6) scaffold: a promising bioactive material for bone tissue engineering, Acta Biomater. (2010), https://doi.org/10.1016/j.actbio.2009.12.022.

[137] C. Wu, J. Chang, J. Wang, S. Ni, W. Zhai, Preparation and characteristics of a calcium magnesium silicate (bredigite) bioactive ceramic, Biomaterials 26 (2005) 2925–2931.

[138] G. Wang, Z. Lu, D. Dwarte, H. Zreiqat, Porous scaffolds with tailored reactivity modulate in-vitro osteoblast responses, Mater. Sci. Eng. C 32 (2012) 1818–1826.

[139] D.C. Clupper, L.L. Hench, J.J. Mecholsky, Strength and toughness of tape cast bioactive glass 45S5 following heat treatment, J. Eur. Ceram. Soc. 24 (2004) 2929–2934.

[140] J. Kim, D. Lim, Y.H. Kim, K. Young-Hag, M.H. Lee, I. Han, S.J. Lee, O.S. Yoo, H.-S. Kim, J.-C. Park, A comparative study of the physical and mechanical properties of porous hydroxyapatite scaffolds fabricated by solid freeform fabrication and polymer replication method, Int. J. Precis. Eng. Manuf. 12 (2011) 695–701.

[141] S. Flauder, R. Sajzew, F.A. Müller, Mechanical properties of porous β-Tricalcium phosphate composites prepared by ice-templating and poly (ε-caprolactone) impregnation, ACS Appl. Mater. Interfaces 7 (2015) 845–851.

[142] Q.Z. Chen, I.D. Thompson, A.R. Boccaccini, 45S5 Bioglass®-derived glass–ceramic scaffolds for bone tissue engineering, Biomaterials 27 (2006) 2414–2425.

[143] C. Wu, J. Chang, W. Zhai, A novel hardystonite bioceramic: preparation and characteristics, Ceram. Int. (2005), https://doi.org/10.1016/j.ceramint.2004.02.008.

[144] M.V. Reddy, M. Pathak, In vitro biological evaluations of Zn doped CaSiO3 synthesized by sol–gel combustion technique, J. Inorg. Organomet. Polym. Mater. 28 (2018) 2187–2195.

[145] A. Liu, M. Sun, H. Shao, X. Yang, C. Ma, D. He, Q. Gao, Y. Liu, S. Yan, S. Xu, The outstanding mechanical response and bone regeneration capacity of robocast dilute magnesium-doped wollastonite scaffolds in critical size bone defects, J. Mater. Chem. B. 4 (2016) 3945–3958.

[146] Z. Du, H. Leng, L. Guo, Y. Huang, T. Zheng, Z. Zhao, X. Liu, X. Zhang, Q. Cai, X. Yang, Calcium silicate scaffolds promoting bone regeneration via the doping of Mg2+ or Mn2+ ion, Compos. B Eng. 190 (2020), 107937.

[147] C. Wu, Y. Ramaswamy, D. Kwik, H. Zreiqat, The effect of strontium incorporation into CaSiO3 ceramics on their physical and biological properties, Biomaterials 28 (2007) 3171–3181.

[148] Y.-H. Lin, A.K.-X. Lee, C.-C. Ho, M.-J. Fang, T.-Y. Kuo, M.-Y. Shie, The effects of a 3D-printed magnesium-/strontium-doped calcium silicate scaffold on regulation of bone regeneration via dual-stimulation of the AKT and WNT signaling pathways, Mater. Sci. Eng. C (2022), 112660.

[149] F.S. Shirazi, M. Mehrali, A.A. Oshkour, H.S.C. Metselaar, N.A. Kadri, N.A.A. Osman, Mechanical and physical properties of calcium silicate/alumina composite for biomedical engineering applications, J. Mech. Behav. Biomed. Mater. 30 (2014) 168–175.

[150] C. Wu, Y. Ramaswamy, P. Boughton, H. Zreiqat, Improvement of mechanical and biological properties of porous CaSiO3 scaffolds by poly (D, L-lactic acid) modification, Acta Biomater. 4 (2008) 343–353.

[151] X. Chen, J. Ou, Y. Wei, Z. Huang, Y. Kang, G. Yin, Effect of MgO contents on the mechanical properties and biological performances of bioceramics in the MgO–CaO–SiO2 system, J. Mater. Sci. Mater. Med. 21 (2010) 1463–1471.

[152] J. Xie, H. Shao, D. He, X. Yang, C. Yao, J. Ye, Y. He, J. Fu, Z. Gou, Ultrahigh strength of three-dimensional printed diluted magnesium doping wollastonite porous scaffolds, Mrs Commun 5 (2015) 631–639.

[153] T. Lu, J. Wang, X. Yuan, C. Tang, X. Wang, F. He, J. Ye, Zinc-doped calcium silicate additive accelerates early angiogenesis and bone regeneration of calcium phosphate cement by double bioactive ions stimulation and immunoregulation, Biomater. Adv. (2022), 213120.

[154] A.M.M. Amin, A.A.M. El-Amir, G. Karunakaran, D. Kuznetsov, E.M.M. Ewais, In-vitro evaluation of wollastonite nanopowder produced by a facile process using cheap precursors for biomedical applications, Ceram. Int. 47 (2021) 18684–18692.

[155] R. Ge, C. Xun, J. Yang, W. Jia, Y. Li, In vivo therapeutic effect of wollastonite and hydroxyapatite on bone defect, Biomed. Mater. 14 (2019), 65013.

[156] C. Wu, J. Chang, S. Ni, J. Wang, In vitro bioactivity of akermanite ceramics, J. Biomed. Mater. Res. Part A An Off. J. Soc. Biomater. Japanese Soc. Biomater. Aust. Soc. Biomater. Korean Soc. Biomater. 76 (2006) 73–80.

[157] Y. Huang, X. Jin, X. Zhang, H. Sun, J. Tu, T. Tang, J. Chang, K. Dai, In vitro and in vivo evaluation of akermanite bioceramics for bone regeneration, Biomaterials 30 (2009) 5041–5048.

[158] W. Zhang, C. Feng, G. Yang, G. Li, X. Ding, S. Wang, Y. Dou, Z. Zhang, J. Chang, C. Wu, 3D-printed scaffolds with synergistic effect of hollow-pipe structure and bioactive ions for vascularized bone regeneration, Biomaterials 135 (2017) 85–95.

[159] H. Zreiqat, Y. Ramaswamy, C. Wu, A. Paschalidis, Z. Lu, B. James, O. Birke, M. McDonald, D. Little, C.R. Dunstan, The incorporation of strontium and zinc into a calcium–silicon ceramic for bone tissue engineering, Biomaterials 31 (2010) 3175–3184.

[160] J. Ou, Y. Kang, Z. Huang, X. Chen, J. Wu, R. Xiao, G. Yin, Preparation and in vitro bioactivity of novel merwinite ceramic, Biomed. Mater. 3 (2008), 15015.

[161] M. Hafezi, A.R. Talebi, S.M. Miresmaeili, F. Sadeghian, F. Fesahat, Histological analysis of bone repair in rat femur via nanostructured merwinite granules, Ceram. Int. 39 (2013) 4575–4580.

[162] S. Ni, J. Chang, L. Chou, W. Zhai, Comparison of osteoblast-like cell responses to calcium silicate and tricalcium phosphate ceramics in vitro, J. Biomed. Mater. Res. Part B Appl. Biomater. An Off. J. Soc. Biomater. Japanese Soc. Biomater. Aust. Soc. Biomater. Korean Soc. Biomater. 80 (2007) 174–183.

[163] H. Sun, C. Wu, K. Dai, J. Chang, T. Tang, Proliferation and osteoblastic differentiation of human bone marrow-derived stromal cells on akermanite-bioactive ceramics, Biomaterials 27 (2006) 5651–5657.

[164] E. O'Neill, G. Awale, L. Daneshmandi, O. Umerah, K.W.-H. Lo, The roles of ions on bone regeneration, Drug Discov. Today 23 (2018) 879–890.

[165] X. Liu, C. Ding, P.K. Chu, Mechanism of apatite formation on wollastonite coatings in simulated body fluids, Biomaterials 25 (2004) 1755–1761.

[166] S. Palakurthy, P.A. Azeem, K. Venugopal Reddy, V. Penugurti, B. Manavathi, A comparative study on in vitro behavior of calcium silicate ceramics synthesized from biowaste resources, J. Am. Ceram. Soc. 103 (2020) 933–943.

[167] S. Sadeghzade, F. Shamoradi, R. Emadi, F. Tavangarian, Fabrication and characterization of baghdadite nanostructured scaffolds by space holder method, J. Mech. Behav. Biomed. Mater. 68 (2017), https://doi.org/10.1016/j.jmbbm.2017.01.034.

[168] F. Soleymani, R. Emadi, S. Sadeghzade, F. Tavangarian, Applying baghdadite/PCL/chitosan nanocomposite coating on AZ91 magnesium alloy to improve corrosion behavior, bioactivity, and biodegradability, Coatings 9 (2019), https://doi.org/10.3390/coatings9120789.

[169] F. Agostinacchio, X. Mu, S. Dirè, A. Motta, D.L. Kaplan, In situ 3D printing: opportunities with silk inks, Trends Biotechnol. 39 (2021) 719–730.

[170] Z. Zhu, D.W.H. Ng, H.S. Park, M.C. McAlpine, 3D-printed multifunctional materials enabled by artificial-intelligence-assisted fabrication technologies, Nat. Rev. Mater. 6 (2021) 27–47.

[171] X. Wang, J. Fang, W. Zhu, C. Zhong, D. Ye, M. Zhu, X. Lu, Y. Zhao, F. Ren, Bioinspired highly anisotropic, ultrastrong and stiff, and osteoconductive mineralized wood hydrogel composites for bone repair, Adv. Funct. Mater. 31 (2021), 2010068.

[172] G. Liu, Y. Zhao, G. Wu, J. Lu, Origami and 4D printing of elastomer-derived ceramic structures, Sci. Adv. 4 (2018) eaat0641.

[173] H. Hwangbo, H. Lee, E.J. Roh, W. Kim, H.P. Joshi, S.Y. Kwon, U.Y. Choi, I.-B. Han, G.H. Kim, Bone tissue engineering via application of a collagen/hydroxyapatite 4D-printed biomimetic scaffold for spinal fusion, Appl. Phys. Rev. 8 (2021), 21403.

[174] Z. Rong, C. Liu, Y. Hu, 4D printing of complex ceramic structures via controlling zirconia contents and patterns, in: Int. Manuf. Sci. Eng. Conf., American Society of Mechanical Engineers (ASME), 2021. V001T01A017.